Nonlinear chemical dynamics

Francesc Sagués [a] and Irving R. Epstein [b]

[a] Departament de Química Física, Universitat de Barcelona, Diagonal 647, E-08028, Barcelona, Spain. E-mail: f.sagues@qf.ub.es

[b] Department of Chemistry and Volen Center for Complex Systems, MS 015, Brandeis University, Waltham, MA 02454, USA

The interdisciplinary field of nonlinear chemical dynamics has grown significantly in breadth and depth over the past three decades. Its subject matter and applications encompass all branches of chemistry as well as areas of mathematics, physics, biology and engineering. In this Perspective, we present an overview of some of the key results of nonlinear chemical dynamics, with emphasis on those areas most likely to be of interest to inorganic chemists. We discuss the range of phenomenology from chemical oscillation to chaos to waves and pattern formation, as well as experimental methods, mechanistic considerations, theoretical techniques, and the results of coupling and external forcing.

Introduction

Many of the most exciting recent developments in chemistry involve the phenomenon of self-organization, the spontaneous emergence of complex, coherent, often periodic, structure involving many molecular units. Inorganic chemistry has been well represented in this area.[1] The study of how complex structure arises, both in time and in space, is a major focus of the field of nonlinear dynamics. In this Perspective, we present a brief overview of nonlinear chemical dynamics, which has been much influenced by inorganic chemistry and which, we believe, has much to offer inorganic chemists. Those who seek a more detailed, chemically oriented, introduction to this area are referred to several monographs and collections of review articles.[2] A more mathematical, but still accessible, treatment may be found in the book by Strogatz.[3]

Like many of the newest areas in science, nonlinear dynamics is highly interdisciplinary and is characterised by a cooperative interplay between theory and experiment. Applications and examples can be found in nearly all fields of chemistry as well as in engineering, mathematics, physics, biology, geology, astronomy, psychology and economics. While most of the early work was in pure theory, the past decade has seen many instances of new experimental breakthroughs inspiring new theoretical and computational approaches and *vice versa*. The phenomena involved are occasionally counterintuitive and often aesthetically pleasing.

Nonlinear dynamics in chemical systems

Nonlinear dynamics is the study of how systems whose behaviour depends in a nonlinear fashion on the values of key variables, like concentrations in a chemical reaction, evolve in

Francesc Sagués graduated in Chemistry and later on received his Ph.D. from Universitat de Barcelona in 1983. In the same year and from the same University he completed graduate studies in Physics. He was a Fulbright postdoctoral fellow at the Physics Department, University of Texas at Austin in 1985–86. He is presently Professor of Physical Chemistry at the Chemistry Department of Universitat de Barcelona. He serves on the steering committee of the European Science Foundation programme on "Stochastic Dynamics: Fundamentals and Applications". His current research interests include the study of nonlinear dynamics, patterns and noise effects in nonequilibrium chemical systems and in complex self-assembling fluids.

Francesc Sagués
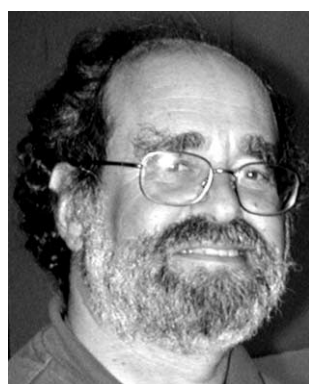
Irving R. Epstein received his A.B. (1966), M.A. (1968) and Ph.D. (1971) degrees from Harvard University. He was a Marshall Scholar at Balliol College, Oxford, in 1966–67, receiving a Diploma in Advanced Mathematics, and a NATO postdoctoral fellow at the Cavendish Laboratory, Cambridge in 1971, before joining Brandeis University, where he is Professor of Chemistry and has served as Dean of Arts and Sciences (1992–94) and Provost and Senior Vice President for Academic Affairs (1994–2001). He has been the recipient of Guggenheim and Humboldt Fellowships and chaired the first Gordon Research Conference on Chemical Oscillations. He serves on the Editorial Board of Chaos *and on the Board of Directors of the New England Complex Systems Institute. His current research interests include nonlinear dynamics, pattern formation and neuroscience.*

Irving R. Epstein
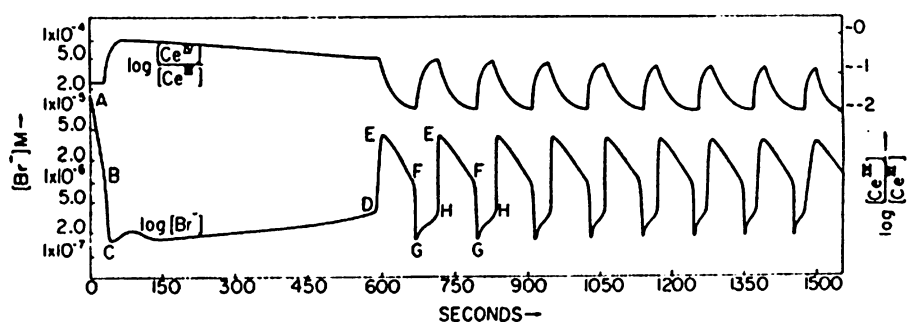
Fig. 1 Oscillatory behaviour in the BZ reaction, showing induction period (A–D) followed by periodic oscillation in the concentrations of several species. Reproduced with permission from ref. 16. Copyright 1972 American Chemical Society.
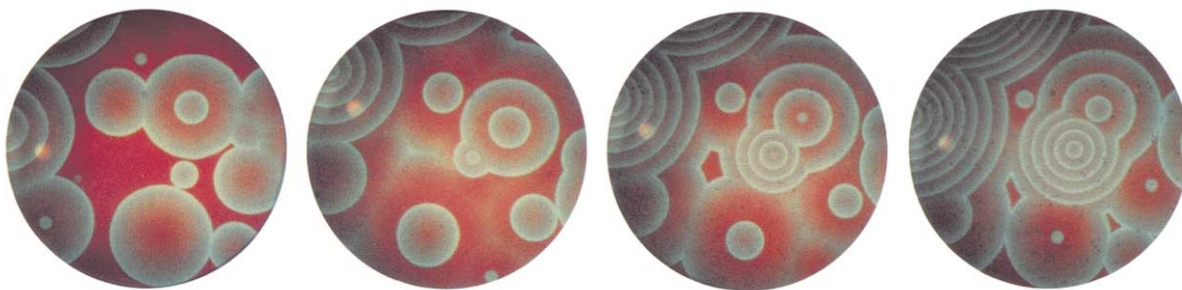
Fig. 2 Target patterns in the BZ reaction. Four successive snapshots taken after reaction evolves from initially homogeneous red (dark) solution. The diameter of each snapshot is about 10 cm.

time. Nearly all systems of interest, including living ones, are nonlinear, often extremely so, but scientists often find it convenient, *e.g.*, in the case of relaxation kinetics,[4] to utilise conditions where the system under consideration behaves linearly. Linear mathematics is familiar and tractable, but it cannot generate even a small fraction of the rich phenomenology of which the "simplest" of nonlinear systems is capable. In chemical systems, nonlinearities typically arise from the rate equations of mass action kinetics; unless one works under special conditions, any bimolecular elementary steps lead to quadratic terms in the rate law. As the example of relaxation kinetics illustrates, if a system is near equilibrium, nonlinear effects may be negligible. It is only far from equilibrium that chemical systems become interesting from the point of view of nonlinear dynamics.

Chemical oscillation

The prototypical phenomenon of nonlinear chemical dynamics is chemical oscillation, the temporally periodic, or nearly periodic, variation of the concentrations of one or more species in a reaction. While reports of electrochemical oscillation date back to 1828,[5] the prevailing wisdom among chemists as late as the 1970s was that chemical oscillation was impossible, a violation of the Second Law of Thermodynamics. Indeed, during the first half of the twentieth century, Bray's report[6] of the first homogeneous chemical oscillator, the iodate-induced decomposition of hydrogen peroxide, generated more articles devoted to debunking it than to explaining it mechanistically.[7]

If chemical oscillation is the prototypical phenomenon, then the Belousov–Zhabotinsky (BZ) reaction is the prototype system for nonlinear chemical dynamics. Like the Bray reaction, the BZ reaction was discovered accidentally, in this case by the Russian chemist B. P. Belousov in the 1950s. Belousov's original reaction mixture consisted of bromate, citric acid and ceric ion. Expecting to observe a monotonic change from yellow Ce^{4+} to colorless Ce^{3+}, he was astonished to find that, after vanishing initially, the yellow color reappeared at about one minute intervals. Skeptical reviewers prevented publication of Belousov's results (despite the inclusion of recipes and photographs) except for one brief note[8] in an unrefereed conference proceeding. A decade later, Zhabotinsky developed the reaction further

and succeeded in publishing his results on several variants of Belousov's original reaction.[9] Zhabotinsky replaced the citric acid with malonic acid, $CH_2(CO_2H)_2$, which has become the standard BZ substrate, though many species with an acidic hydrogen alpha to two electron-withdrawing groups also generate oscillation, with different pre-oscillatory induction periods, amplitudes and periods of oscillation. In addition to the color change, oscillations may be observed in the redox potential (primarily determined by the ratio of the oxidised and reduced forms of the metal ion) and the bromide ion concentration as well as in the concentrations of several organic intermediates.[10] Typical data are shown in Fig. 1.

The cerium, which serves as a catalyst, can be replaced by other metal ions or complexes with similar one-electron redox potentials. Two catalysts in particular, ferroin $[Fe(phen)_3^{2+}]$ and Rubipy $[Ru(bipy)_3^{2+}]$,[11] deserve special mention. Ferroin, originally used by Belousov as a redox indicator to enhance the color changes in the cerium-catalysed system, was shown by Zhabotinsky to be capable of acting on its own as a catalyst. In an unstirred thin (*ca.* 1 mm deep) layer, the ferroin-catalysed BZ system generates striking spatial patterns consisting of spirals or concentric rings (target patterns)[12] like those illustrated in Fig. 2. The spontaneous growth of blue rings or spirals in an initially homogeneous dish of red solution is a remarkable phenomenon, serving as both an inspiring lecture demonstration and an intriguing analogue of patterns seen in biological systems such as aggregating slime moulds[13] or developing frog oocytes.[14] The Rubipy catalyst is photosensitive and affords the possibility of perturbing and controlling either the temporally oscillating stirred system or the spatially patterned unstirred system with considerable precision.[15] Some applications of this powerful tool are discussed below.

In the early 1970s, Field, Körös and Noyes[16] (FKN) combined kinetic and thermodynamic approaches to propose a detailed mechanism for the BZ reaction. Using what at the time represented state-of-the-art numerical analysis and computing capabilities, they were able to simulate the resulting rate equations and demonstrate that oscillatory behaviour was indeed obtained.[17] Together with theoretical advances in nonequilibrium thermodynamics,[18] the FKN mechanism provided the chemical community with the evidence it needed to consider

chemical oscillation a legitimate phenomenon deserving of careful study. The problem remained, however, that aside from living systems and the serendipitously discovered Bray and BZ reactions and their variants, there were no other chemical oscillators and no systematic route toward creating them. Fortunately, a solution to that problem was soon forthcoming.

Combining a generic mathematical model,[19] a continuous flow stirred tank reactor to maintain the system far from equilibrium,[20] and some inorganic reaction kinetics,[21] De Kepper, Kustin and Epstein[22] constructed the first systematically designed chemical oscillator, the chlorite–iodate–arsenite reaction. Their approach is based on the following principles:

(1) Sustained oscillation can occur only if a system is maintained far from equilibrium. One way to do this is to run the reaction in a flow reactor, which allows for continuous input of fresh reactants and outflow of products.

(2) Autocatalytic reactions frequently exhibit bistable behaviour when run in a flow reactor. That is, for certain sets of input concentrations and flow rate, the system may, depending upon its history, reach either of two steady states, each of which is stable to small perturbations.

(3) If a bistable system is subjected to a feedback that affects the concentration of the autocatalytic species on a time scale long with respect to the characteristic times for the system to relax to its steady states, then by intensifying the feedback, it should be possible to cause the system to oscillate, essentially between the two, no longer stable, steady states.

(4) The situation described above can be generated by choosing an autocatalytic reaction, running it in a flow reactor to determine conditions for bistability, and then adding a feedback species that reacts sufficiently slowly with the appropriate species in the autocatalytic reaction. Increasing the concentration of the feedback species in the input flow should bring the system into its oscillatory state.

This scheme eventually proved so successful that the repertoire of chemical oscillators has grown from two accidentally discovered systems and their variants to literally dozens of new oscillating reactions spanning much of the periodic table. While oxyhalogen chemistry,[23] which characterises both the Bray and the BZ systems, remains the richest source, sulfur,[24] phosphorus,[25] cobalt[26,27] and manganese chemistry[28] as well as organic reactions[26] also give rise to significant numbers of oscillating reactions. Mechanisms have been developed for many chemical oscillators, making it possible to identify families of oscillators and even "minimal oscillators,"[29] *i.e.*, the unique member of a family whose components are found, either as reactants or as intermediates, in all members of that family. In Fig. 3 we present a "taxonomy" of chemical oscillators, showing the major families and the links between them, reactions that
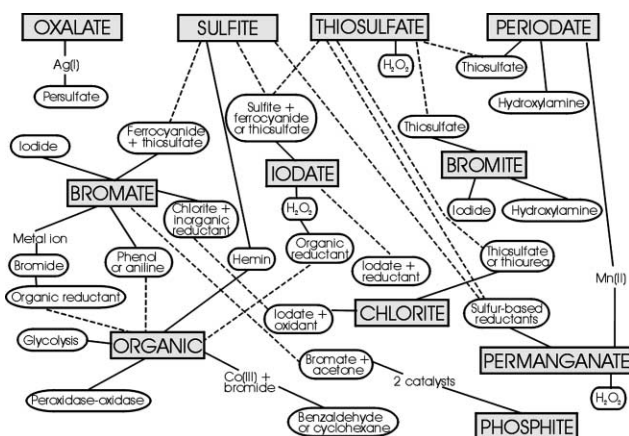
contain components from more than one family. The complexity of this picture reflects the richness of the vein of oscillatory behaviour that has been tapped over the past two decades.

Multistability

The phenomenon of bistability played a major role in the systematic design of chemical oscillators. More generally, multistability, the existence of two or more stable dynamical states (steady state, periodic oscillation, chaos) of a system under the same set of external constraints—input concentrations of reactants, temperature, pressure, *etc.*—is one of the most interesting and significant phenomena in nonlinear dynamics. Multistability can occur only in open systems subject to a flow of reactants and/or energy, since a closed system possesses a unique equilibrium state. Its simplest manifestation is bistability, the simultaneous existence of two stable steady states. A bistable system in one of its steady states when subjected to a small (subthreshold) perturbation will relax back to its original state, but a large enough (superthreshold) disturbance will result in a transition to the other steady state. An example of such behaviour in the oxidation of arsenous acid by iodate ion is shown in Fig. 4. This reaction is perhaps the best understood of the many bistable systems that have now been studied, thanks in large measure to the elegant work of Showalter and collaborators.[30] The key reactions, both of which have been known for nearly a century, are the Dushman reaction,[31] in which the intermediate iodine is produced:
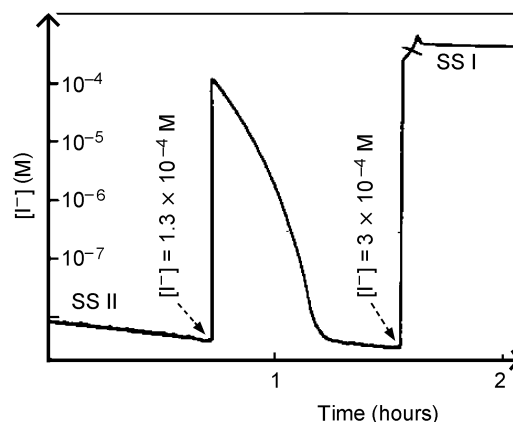
Fig. 4 Bistability in the arsenous acid–iodate reaction. Reaction is carried out in a flow reactor. After steady state (SSII) is established, iodide ion is added as indicated by the arrows. A small addition leads to relaxation back to SSII, while a larger addition causes a transition to the other steady state (SSI). Reproduced with permission from ref. 21. Copyright 1981 American Chemical Society.

$$IO_3^- + 5I^- + 6H^+ = 3I_2 + 3H_2O \qquad (1)$$
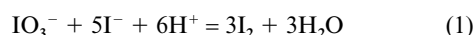
and the Roebuck reaction,[32] in which iodine reacts with arsenous acid to regenerate iodide:

$$I_2 + H_3AsO_3 + H_2O = 2I^- + H_3AsO_3 + 2H^+ \qquad (2)$$

The net reaction, (3) = (1) + 3 × (2), is autocatalytic in iodide ion, since reaction (1) is rate-determining.

$$IO_3^- + 3H_3AsO_3 = I^- + 3H_3AsO_4 \qquad (3)$$
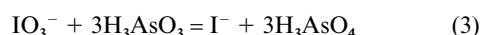
Bistable systems exhibit hysteresis: as a control parameter is slowly varied, the steady state composition of the system changes continuously until, at a critical value of the parameter, the steady state becomes unstable and the system undergoes a jump to the composition characteristic of the other steady state. When the parameter is varied in the opposite direction, the steady state composition again varies smoothly until a second

Fig. 3 A taxonomy of chemical oscillators. Rectangular boxes contain major families. Ovals contain examples of oscillators. Species outside of boxes are catalysts. Solid lines connect members of a family. Dashed lines show some of the links (members in common) between families.

transition point, different from the first, is reached and the system jumps back to the original state. The region of bistability, in which the system can be in either steady state, lies between the two transition points. Bistable systems thus have a memory; the steady state to which they evolve depends upon the composition they start with.

While bistability involving two steady states is the most commonly encountered form of multistability, several other multistable phenomena have been observed in relatively simple inorganic reactions. In many systems, varying a control parameter leads to a subcritical Hopf bifurcation, beyond which a stable steady state coexists with a stable oscillatory state. In the range of coexistence, concentrations remain stationary or oscillate periodically, depending upon the past history of the system. Small perturbations to either the steady or the oscillatory state decay, but larger ones can cause a transition from stationary to periodic behaviour or *vice versa*. Fig. 5 illustrates hysteresis between a steady state and an oscillatory state in the bromate–iodide reaction.[33]
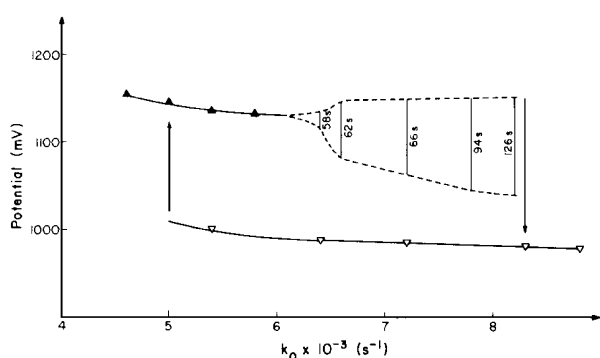
Fig. 5 Hysteresis between steady and oscillatory states in the bromate–iodide reaction. Triangles show steady state values of potential of a Pt redox electrode. Dashed lines show maximum and minimum potential in the oscillatory state, with vertical lines marked by period of oscillation. Upper branch shows data taken at increasing flow rate k_0, lower branch taken at decreasing k_0. Arrows indicate transitions between branches of states. Reproduced with permission from ref. 33. Copyright 1983 American Chemical Society.

Less frequently occurring multistable behaviours include birhythmicity, the coexistence of two stable oscillatory modes, a phenomenon first observed in the bromate–chlorite–iodide reaction,[34] and tristability, in which three stable steady states can occur under the same set of conditions. This latter phenomenon is found in the chlorite–iodate–iodide-arsenous acid[35] and chlorite–iodine–iodide–thiosulfate[36] systems. Recently, De Kepper and coworkers[37] have drawn attention to the phenomenon of *spatial bistability*, in which two different spatial patterns of concentration can occur in an unstirred, spatially extended system under identical conditions, with the selection between them again depending upon the history of the system. Pattern formation in general will be discussed in more detail below.

It is noteworthy that several of the systems that display complex multistable behaviour, such as bromate–chlorite–iodide or chlorite–iodate–iodide–arsenous acid, may be thought of as *chemically coupled*,[38] *i.e.*, as consisting of two reactions, each of which would be bistable or oscillatory on its own, linked through a common intermediate. For example, both the bromate–iodide[33] and chlorite–iodide[39] reactions show oscillatory behaviour, but the coupled bromate–chlorite–iodide system exhibits a far richer range of dynamical behaviour than either of the two uncoupled systems.[34] Chemical coupling is one way of generating multistability. Another is *physical coupling*, in which two or more systems interact through a physical process like diffusion across a membrane. By joining two flow reactors containing the ingredients of the BZ

reaction through an adjustable aperture in a common wall, it is possible to generate bistability between stationary and oscillatory states as well as between oscillatory states in which the oscillations in the two compartments are either in phase or out of phase with each other.[40] By linking more units, one can construct systems with very large numbers of multistable states. Laplante and Erneux[41] studied a linear arrangement of 16 physically coupled, individually bistable chlorite–iodide reactions, which has, in principle, 2^{16} possible states, while Laplante *et al.*[42] used a system of 8 coupled bistable arsenous acid–iodate reactions linked by 16 connecting tubes as a primitive pattern recognition device. Coupling smaller systems to one another provides a powerful route not only to inducing multistable behaviour but also to generating other more complex dynamical phenomena. The related phenomenon of external forcing will be considered later in this article.

Chaos

The concept of chaos has been characterised as one of the major new scientific ideas to emerge from the past century.[43] While it has played a more central role in mathematics and physics, chaotic behaviour is found in many chemical systems as well.[44] To get a sense of chemical chaos, compare the oscillations in Fig. 6 with those in Fig. 1. The EFGH pattern in Fig. 1 repeats regularly with no variation, while in Fig. 6, the pattern consists of small and large peaks alternating in an irregular, apparently random fashion. Chaos in an open chemical system may be defined as an aperiodically varying composition determined by the intrinsic dynamics of the system (rather than by noise or external influences), which depends sensitively on the initial conditions, *i.e.*, two chaotic systems that differ even infinitesimally in their initial conditions evolve in time so as to diverge exponentially from one another. Chaotic behaviour typically emerges from periodic oscillation as a control parameter is varied, often by a period-doubling route,[45] in which alternate extrema become slightly larger or smaller at a series of critical values of the parameter until, at a limit point, the behaviour becomes aperiodic, *i.e.*, chaotic. Fig. 6 shows another form of chaos in the chlorite–thiosulfate reaction.[46]

The first experimental demonstrations of chaos in a chemical system were made on the BZ reaction.[47] Chaotic behaviour has
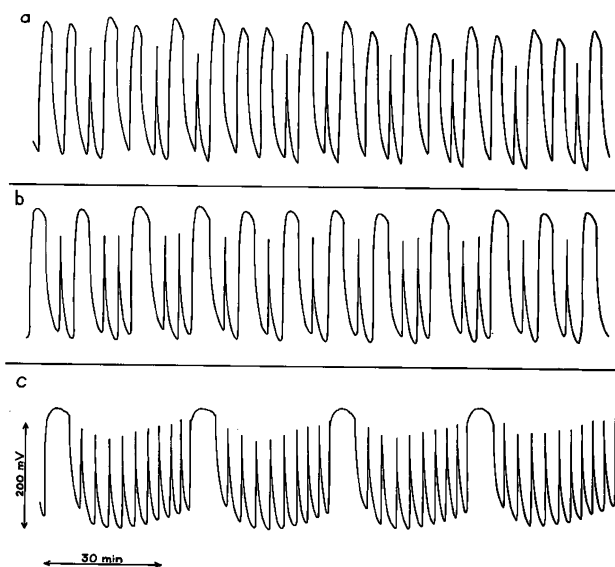
Fig. 6 Chaos in the chlorite–thiosulfate reaction in a flow reactor. Input concentrations, $[ClO_2^-]_0 = 5 \times 10^{-4}$ M, $[S_2O_3^{2-}]_0 = 3 \times 10^{-4}$ M, pH = 4, residence time in reactor = a) 6.8 min, b) 10.5 min, c) 23.6 min. Reproduced with permission from ref. 46. Copyright 1982 American Chemical Society.

subsequently been found in many other systems, including the chlorite–thiosulfate[46] and the hydrogen peroxide–bisulfite–bicarbonate[48] reactions, the cobalt/manganese/bromide-catalysed autoxidations of *p*-xylene and cyclohexanone,[49] the gas phase oxidation of carbon monoxide[50] and the electro-dissolution of copper.[51]

Every chaotic trajectory contains an infinite number of unstable periodic paths, and it has been suggested that one should be able to "control chaos" by applying very small, carefully selected perturbations to a chaotic system in order to stabilise a chosen periodic behaviour.[52] This approach has been put into practice successfully in the BZ system[53] and in gas phase combustion reactions.[54] Another intriguing notion, thus far implemented only in numerical simulations of the BZ reaction, is that sequences of symbols (messages) might be encoded and decoded in the chaotic oscillations of a chemical system using a similar control algorithm.[55]

Patterns and waves

Perhaps the most significant, and certainly the most visually striking, phenomenon associated with nonlinear dynamics in reaction–diffusion systems is the spontaneous appearance of propagating waves and spatial patterns. Watching an apparently homogeneous dish of unstirred solution give birth to the sort of pattern shown in Fig. 2 has inspired many a student to pursue further study of chemistry and of nonlinear dynamics.

The simplest phenomenon of this sort is a propagating front, which divides a system into two regions in different states, *e.g.*, reacted and unreacted. Such a front is typically quite narrow and moves with nearly constant velocity. This type of behaviour is common in autocatalytic reaction–diffusion systems as well as in the movement of wind-driven forest fires, expanding bacterial colonies, advancing regions of corrosion or the spread of infectious diseases. Simple autocatalytic models with quadratic or cubic nonlinearities have been thoroughly analysed[56] and shown to support front propagation. In addition to the arsenous acid–iodate[30] reaction, front behaviour has been investigated experimentally in the reactions of chlorite and sulfite,[57] ferroin and bromate,[58] and Fe(II) and nitric acid.[59] Szirovicza *et al*.[60] have developed an algorithm for constructing systems that support pH fronts in acid- and base-catalysed autocatalytic reactions.

When the system is oscillatory or excitable, more complex behaviour can arise. By excitable we mean that the system has a stable steady state that when perturbed by a small amount quickly returns to its initial concentrations, but perturbations that exceed a threshold first grow before the system relaxes back to the original state. Such excitable media occur not only in chemical systems but also in biological contexts, such as nerve cells and heart muscle.[61] Instead of a simple front, one observes either a single pulse or a series of pulses, in which the concentrations are at one level before and after the pulse and at a different level within the pulse, which has fronts both ahead of and behind it ("wave front" and "wave back"). After a refractory period that follows the passage of a pulse, the medium can support another pulse. It is thus possible to have a train of pulses, which in two dimensions can result in a pattern of concentric rings (target pattern) like those in Fig. 2 or, if a ring is broken, spirals. Spiral waves are seen not only in homogeneous reaction–diffusion systems, but also in heterogeneous catalysis. The most thoroughly characterised catalytic system is the oxidation of CO on the 110 surface of a Pt single crystal, a reaction which shows not only target patterns and spirals,[62] but a rich array of more complex patterns as well.[63]

We can expand the variety of wave propagation phenomena considerably if we go from two-dimensional to three-dimensional systems. The simplest structures in this situation correspond to the 3D extension of 2D target patterns and spiral waves. These are respectively referred to as spherical and scroll waves.[64] In the latter case, one easily imagines a set of spirals stacked on top of each other. The tips of the spirals will now be organized around a column of cores composing a circular tube or filament. In the simplest situation, one can envisage a straight filament, but the filament may also twist or bend. Still more complex shapes are possible if we allow the filament to close on itself, generating scroll rings or even knots. We stress that scroll rings, in contrast to the commonly found steady rotating spirals, are not stable, since they possess a vertical drift along their symmetry axis superposed on a collapsing (at moderate excitability) or expanding (at weak excitability) dynamics. Strogatz and Winfree[65] have exhaustively analysed, using geometric and topological arguments, an impressive variety of three-dimensional waves, extracting precise topological requirements that must be satisfied in order for these waves to be compatible with physico-chemical principles. Apart from their interest in a chemical context, spiral and scroll waves have been observed in many different scenarios of excitability. In particular, biological realizations of excitable systems can be found in neuronal and heart tissue,[66] in the latter case suggesting striking similarities between scroll waves and cardiac arrhythmias.[67]

The patterns described above are nonstationary; regions of different concentrations move through space. Another important class of patterns, with potential implications for biological, geological and other systems as well as in chemistry, are stationary; once formed, they remain fixed in space. Stationary patterns in reaction–diffusion systems are associated with the seminal work of Turing[68] in 1952. He proposed that, as a result of diffusion coupling to nonlinear kinetics, a uniform steady state that is stable to homogeneous perturbations could become unstable to spatially nonuniform disturbances. It would thus be transformed to another stable, temporally stationary but spatially patterned state, now referred to as a Turing pattern. Turing patterns were widely embraced by theoretical biologists as a model for pattern formation in living organisms,[69] but it was not until nearly four decades after Turing's death that the first experimental evidence of Turing pattern formation was obtained, in the chlorite–iodide–malonic acid (CIMA) reaction.[70] The experimental elusiveness of Turing patterns results from the need to have two species with very different diffusivities, a requirement not easily satisfied in aqueous solution. The CIMA reaction turns out to be a fortuitous choice, because the starch indicator used in the gel reactor in which the experiments were done reversibly forms an immobile complex with triiodide, thereby slowing the effective diffusion rate of the key iodine species by about an order of magnitude.[71] This observation suggests an approach to designing additional Turing pattern-forming systems by appropriate choices of reactions and complexing agents.[72] Examples of Turing patterns in the CIMA reaction, with their characteristic striped and hexagonal (spotted) structures[73] are shown in Fig. 7. The patterns, particularly the hexagonal structure in the left panel of Fig. 7, suggest a sort of two-dimensional crystal, and model calculations[74] imply that three-dimensional patterns should arrange them-
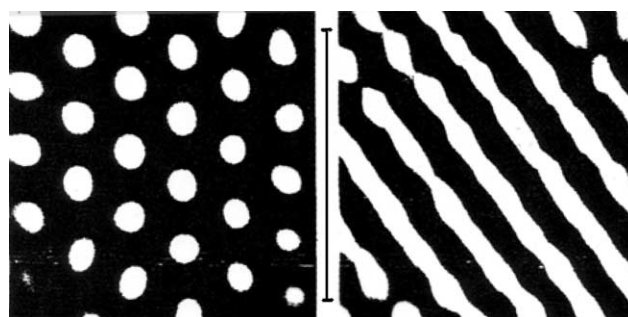

Fig. 7 Turing patterns in the chlorite–iodide–malonic acid reaction. Dark areas show high concentrations of starch–triiodide complex. Length of vertical bar = 1 mm.

selves in ways resembling the packing of atoms or molecules in a crystal, though experiments on three-dimensional Turing patterns still remain to be done.

Quite recently, the Brandeis group has developed a new system, a water-in-oil reverse microemulsion with nanometer-sized droplets of water surrounded by a monolayer of the surfactant sodium bis(2-ethylhexyl)sulfosuccinate (AOT) dispersed in oil (octane), for studying pattern formation. When the reactants of the BZ reaction are introduced into this medium (BZ–AOT system), a remarkable array of pattern formation, summarised in Fig. 8, results. In addition to Turing patterns, previously unobtainable in the BZ reaction, one observes targets and spirals, standing waves, and clusters, which consist of regions that oscillate in time but remain stationary in space, and several phenomena that are seen for the first time in the BZ–AOT medium. These include waves that appear to accelerate as they approach one another and then go off at right angles after collision,[75] in contrast to BZ waves in other media, which move with constant velocity and annihilate on collision; wave packets,[76] which resemble electromagnetic waves; antispirals,[77] which move toward rather than away from their centers; and dash-waves,[78] which consist of alternating regions of active and quiescent medium. The extraordinary versatility of the BZ–AOT system stems from two properties: a) the size and spacing of the water droplets can be controlled by varying the concentrations of water, oil and surfactant; and b) most of the species in the BZ reaction are polar and therefore reside in the water droplets, diffusing at a relatively slow rate characteristic of entire droplets, while some key intermediates, notably Br_2 and BrO_2, are non-polar and therefore escape into the oil and are able to diffuse much more rapidly. More detailed investigations of this fascinating system, including its use with other reactions, are planned.
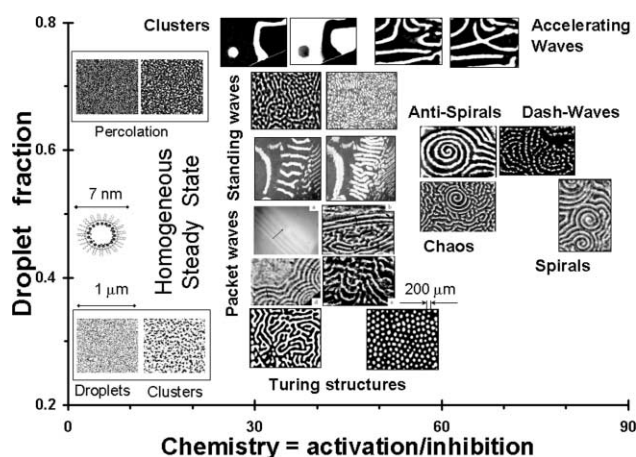

Fig. 8 Summary of dynamical behaviour in the BZ–AOT microemulsion system. "Droplet fraction" is the volume fraction of the medium occupied by water droplets.

Interaction with external influences

We have described above the behaviour of nonlinear reaction–diffusion systems in the absence of external forces. Chemists, of course, have always been fond of subjecting their reactions to light, heat or other influences in order to understand them more deeply or to get them to perform in desired ways. Nonlinear systems are sensitive to external influences, sometimes exquisitely so, and even the effects of gravitational and magnetic fields can be significant. Here we survey briefly some of the phenomenology of external forces interacting with nonlinear dynamics.

Bazsa and Epstein[59] demonstrated that fronts in the oxidation of iron (II) by nitric acid can propagate as much as six times faster down a vertical tube than up the same tube. This anisotropy, clearly gravitationally driven, can be decreased or

eliminated either by using a wider tube or by adding silica gel to the reaction mixture. In the chlorite–thiosulfate system, either ascending or descending fronts may travel faster, depending upon the concentrations of reactants.[79] Pojman and Epstein[80] subsequently developed a theory of anisotropic velocity behaviour in propagating fronts based on the phenomenon of double-diffusive convection, which occurs when "salt fingers" occur in a body of water containing hot, salty water above cold, fresh water. In the chemical system, there are two sources of density change as the reaction proceeds: the change in composition and the exothermicity.[81] The former may cause the density of the product solution to be either greater or less than that of the unreacted solution; for example, in the oxidation of ferrous ion by nitric acid, the higher charge on the product ferric ion apparently pulls in the solvent molecules more tightly and causes the solution density to increase. Thermal effects always cause the density to decrease as the reaction proceeds. Also, differences in temperature spread much more rapidly than do differences in concentration and are dissipated more rapidly in thin tubes than in thick ones. The interplay of these features leads to an understanding of the complex effects of gravitational fields on propagating fronts.

Buoyancy effects can play an even more crucial role, since in addition to affecting the propagation of preexisting waves or fronts, they can generate instabilities leading to pattern formation in chemical systems. Chemoconvective patterns, *i.e.*, patterns originating from hydrodynamic motions triggered by chemical reactions, have been extensively studied.[82] One particularly interesting example is the so-called "blue bottle" reaction,[83] the alkaline glucose reduction of methylene blue. Upon standing, the solution turns colorless following the reduction of the indicator by glucose. After the sample is shaken, the blue color reappears, indicating that the methylene blue is oxidised by atmospheric oxygen. When the reaction takes place in an open Petri dish, an overturning instability, apparently caused by the accumulation of the slightly denser product, gluconic acid, at the upper surface, occurs. This hydrodynamic instability is made visible by the presence of blue dots or lines in regions of downwelling fluid.[84,85] Recently, gravity effects have also been observed in waves of spreading depression in the retina.[86]

The effects of relatively modest electric and magnetic fields on chemical reactions are generally thought to be negligible, though there have been questions raised recently as to the consequences for human health of fields from power lines and computer terminals,[87] and some animals are able to use even the earth's tiny magnetic field for navigation.[88] Certain nonlinear chemical reactions appear to be ideally suited for probing the effects of moderate electric and magnetic fields. Since several of the key intermediates in the BZ reaction are ionic, it seems plausible that an applied electric field might modify propagation of BZ waves. A number of investigators have demonstrated that this is indeed the case. The most thorough studies have been done by Marek and collaborators,[89] who showed that fields of the order of 10–50 V cm^{-1} have significant effects on wave propagation. For, example, if the field is configured so that the front propagates toward the positive electrode, a constant field of 20 V cm^{-1} accelerates the front from 2.3 to 5.7 mm min^{-1}. Doubling the field yields waves propagating as much as five times faster than in the field-free situation. Reversing the direction of the field produces even more dramatic effects. At small fields, propagation is slowed, as one might expect. For fields between 10 and 20 V cm^{-1}, new waves split off from the original wave and travel in the opposite direction. At still higher fields, the initial wave is annihilated and replaced by a backward-moving wave. These effects are attributable primarily to the movement of bromide ions, which inhibit the reaction, toward the positive electrode. Model calculations that take into account both the mobility of the ionic species and the effects on the local electric field as a result of the varying

concentration profiles of these species provide a more detailed understanding.[90]

Electric field effects also give rise to more complicated wave propagation phenomena. Experiments have been performed on spiral excitation patterns in the BZ reaction under the influence of an externally applied direct current.[91] The spirals drift at a rate that depends on the intensity of the applied electric field and in a direction that may be decomposed into a component parallel to the electric field (pointing toward the positive electrode) and a perpendicular component whose sign depends on the chirality of the spiral. More complicated scenarios are also possible, such as "super-spirals", resulting from rapid tip meander induced by pulses of electrical current applied at the tip.[92] The possibility of annihilating spirals by moving a pair toward each other by means of electric fields has also been investigated.[93]

More surprising than the effects of electric fields on wave propagation are those of magnetic fields. Fig. 9 shows how a circular wavefront in the Co(II)-catalysed autoxidation of benzaldehyde is distorted as it spreads in a magnetic field of maximum strength 0.6 T.[94] The front is accelerated by as much as a factor of five as it proceeds into regions of decreasing field strength and is stopped by positive field gradients. Note that the initial solution containing Co(II) is paramagnetic, while Co(III) is diamagnetic.
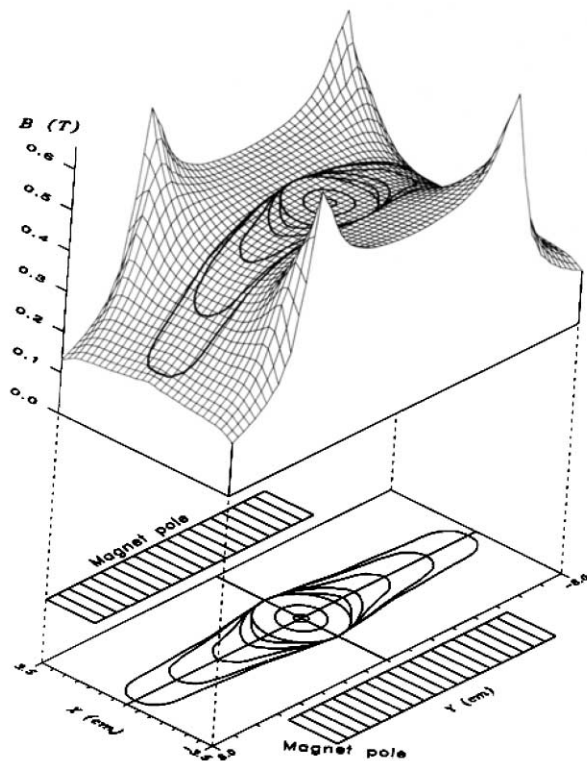

Fig. 9 Magnetic field effects. (Top) Magnetic field strength B in the central horizontal plane of two flat 10 cm diameter cylindrical magnets placed 8 cm apart. (Bottom) Time development of a wavefront in a solution containing benzaldehyde and cobalt(II) acetate in oxygen-saturated glacial acetic acid as it spreads in this quasi-two-dimensional system. Reprinted by permission from Nature (ref. 94), copyright 1990 Macmillan Publishers Ltd.

Temperature, of course, plays a major (and nonlinear, *via* the Arrhenius factor, which, in an exothermic reaction, generates a form of autocatalysis) role in determining the rates of chemical reactions. Chemists studying nonlinear dynamics in homogeneous systems have, for the most part, worked under isothermal conditions,[95] in part because most chemical oscillators operate only over a relatively narrow range of temperatures, in part to avoid introducing another set of parameters, the activation energies, into their modeling efforts. Chemical engineers

interested in heterogeneous reactions, especially those catalysed by metal surfaces, have devoted more attention to the role played by temperature changes and to the potential for using temperature as a parameter to control and to probe the behaviour of thermokinetic oscillators.[96] Temperature oscillations in some catalytic oscillators can reach amplitudes of hundreds of degrees.[97]
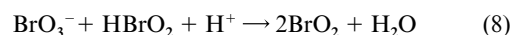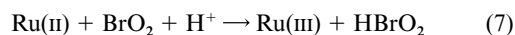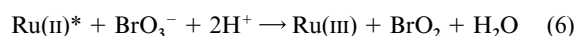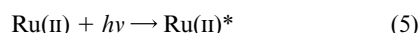
Temperature gradients have sizeable effects on the propagation of waves under oscillatory and excitable conditions. This principle was cleverly employed[98] to precisely orient scroll rings in space and to modify their lifetimes by accelerating, decelerating, or even reversing their spontaneous shrinkage. This striking result, together with those reported above on the effects of electric fields on spirals, can be rationalized in terms of kinematic descriptions of the wave dynamics.[99]

Certainly the most extensively studied external influence on nonlinear reaction-diffusion systems has been light. Even an apparently simple reaction like the decomposition of $S_2O_6F_2$:

$$S_2O_6F_2 \rightleftharpoons 2SO_3F \qquad (4)$$
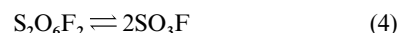
when illuminated displays a rich set of phenomena, including bistability under constant illumination,[100] and tristability, oscillations, and chaos when a delayed feedback[101] is applied to modulate the intensity of the incident light.[102]

The Rubipy-catalysed BZ reaction is quite photosensitive, owing to the formation of excited catalyst molecules, which produce the autocatalyst, bromine dioxide:[103]

$$Ru(II) + h\nu \longrightarrow Ru(II)^* \qquad (5)$$

$$Ru(II)^* + BrO_3^- + 2H^+ \longrightarrow Ru(III) + BrO_2 + H_2O \quad (6)$$

$$Ru(II) + BrO_2 + H^+ \longrightarrow Ru(III) + HBrO_2 \qquad (7)$$

$$BrO_3^- + HBrO_2 + H^+ \longrightarrow 2BrO_2 + H_2O \qquad (8)$$

This tool has been exploited to store photographic images on the surface of a solution containing the BZ reactants.[15] Under excitable conditions, control of illumination has been used to change the frequency of rotating spirals,[104] to split waves using pulsed illumination,[105] to cause spirals to drift in a gradient[106] or with periodic modulation[107] of the light intensity, and to control wave motion *via* feedback.[108,109] In three-dimensional systems, eventual control of turbulent regimes for scroll waves under periodic temporal modulation has been recently considered both numerically and analytically.[110] In the oscillatory regime, signatures of resonant pattern formation have been detected under periodic forcing,[111] and feedback control has been used to generate cluster patterns, in which different regions of the medium oscillate with different phase.[112]

In addition, the light-sensitive BZ reaction opens up a wide field of research dealing with the effect of disordered patterns of excitability on different scenarios of wave propagation. This has been a major interest of the Barcelona group in recent years. Randomness in the illumination is easily introduced, either by applying a homogeneous but temporally fluctuating light intensity or by projecting a random, spatiotemporally patterned illumination. A number of striking results have been experimentally observed, reproduced numerically and analytically interpreted. The main observations can be classified into two groups. In the first, noise-induced transitions from sub-excitable to excitable,[113,114] and from excitable to oscillatory regimes have been observed.[114] Spatially extended, temporally varying noise of zero average, superposed on a mean value of illumination that corresponds to no wave propagation (resp. single wave propagation) is able to generate single wave propagation (resp. target patterns). Fig. 10 shows experimental observations of the excitable to oscillatory transition, where the upper row of snapshots follows a single ring developing in the
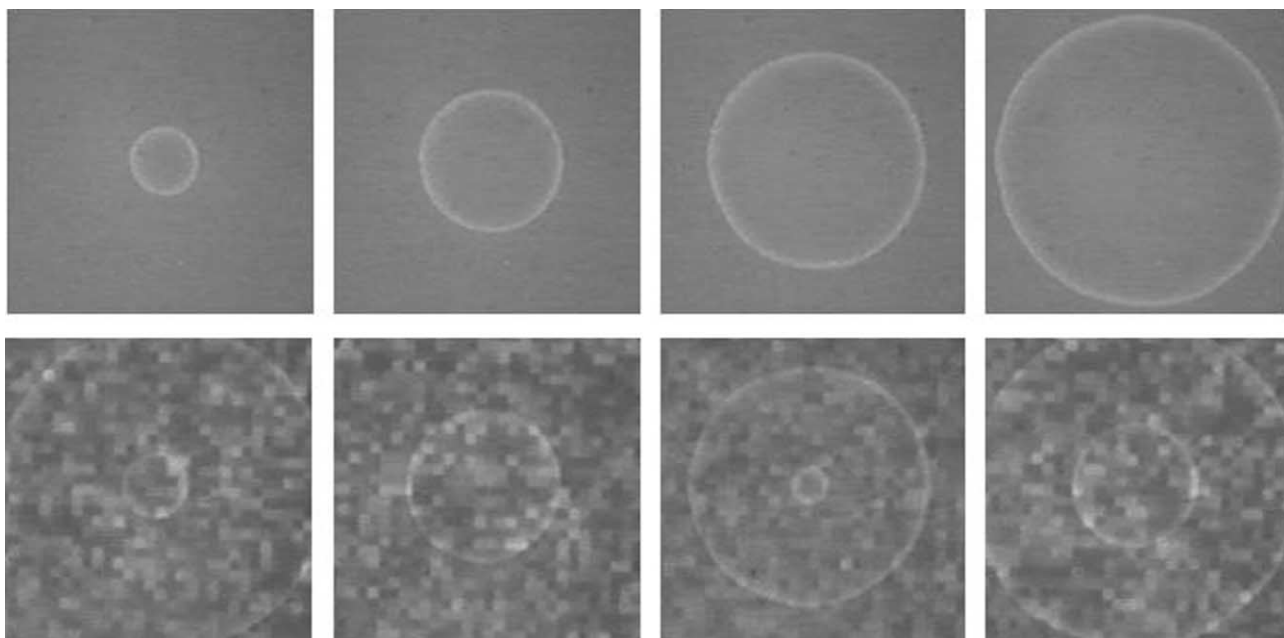
Fig. 10 Excitable to oscillatory transition mediated by spatiotemporal noise of zero mean superimposed on a constant level of illumination in the photosensitive BZ reaction. From ref. 114.
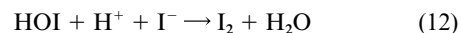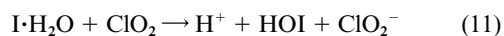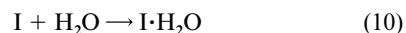
absence of noise, and the lower row demonstrates how a second ring, the precursor of a target pattern, is induced by the random illumination. In the second class of problems, zero-mean randomness in the illumination is used to force preexisting patterns. The simplest case corresponds to a single front[115] perturbed by frozen disorder, where we observe accelerating or retarding effects, depending on the dimensionality of the pulse. More interesting is our observation of the Brownian dispersion of spiral waves (Fig. 11), which shows pronounced resonant effects when the system is forced with spatially patterned and time-correlated noise.[116] This last situation was also explored in relation to the lifetime of collapsing scroll rings.[117]
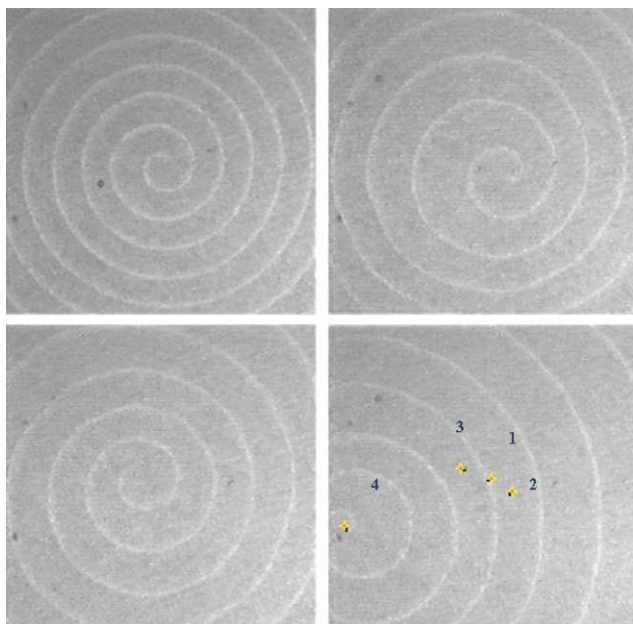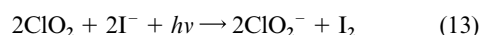

Fig. 11 Brownian motion of spirals induced by spatiotemporal noise of zero mean superimposed on a constant level of illumination in the photosensitive BZ reaction. From ref. 116.

Another photosensitive system that has been of considerable importance in nonlinear chemical dynamics is the CIMA reaction and the related CDIMA (chlorine dioxide–iodine–malonic acid) reaction. These reactions are the system of choice for

studying Turing patterns and also support a variety of other phenomena such as oscillations, bistability and front propagation.[118] The Brandeis group showed that illumination of the CDIMA system with a tungsten-halogen lamp suppresses oscillations and shifts the steady state to lower concentrations of iodide and triiodide.[119] They attribute this behaviour to the photodissociation of I_2, which leads to a sequence of reactions:

$$I_2 + h\nu \longrightarrow 2I \qquad (9)$$

$$I + H_2O \longrightarrow I \cdot H_2O \qquad (10)$$

$$I \cdot H_2O + ClO_2 \longrightarrow H^+ + HOI + ClO_2^- \qquad (11)$$

$$HOI + H^+ + I^- \longrightarrow I_2 + H_2O \qquad (12)$$

The net reaction is then

$$2ClO_2 + 2I^- + h\nu \longrightarrow 2ClO_2^- + I_2 \qquad (13)$$

By varying the intensity of illumination, one can modify or even suppress the appearance of Turing patterns. Periodic variation of the light intensity is more effective than constant illumination at the same average intensity, and pattern suppression is most effective at a frequency of illumination equal to the frequency of oscillation in a stirred CDIMA system of similar composition.[120] Illuminating a Turing pattern at constant intensity through a spatially patterned mask yields similar resonance-like effects, *i.e.*, illumination is most effective in modifying the pattern when the wavelength of the mask is equal to (or a small integral multiple of) the wavelength of the naturally occurring pattern.[121]

Experimental tools

One of the most remarkable aspects of the development of nonlinear chemical dynamics is that nearly all of the most significant experimental advances have been made with relatively simple equipment; this has traditionally been a low-tech field. Perhaps because even state-of-the-art studies can be done with inexpensive apparatus, nonlinear chemical dynamics has always been a very international field as well, with major contributions coming from investigators in less-developed as well as wealthier nations.

The earliest experiments on oscillating reactions were done in beakers and observed by eye. When more quantitative measurements were called for, potentiometric and spectrophotometric techniques were employed. Platinum redox electrodes are commonly used to monitor reactions in aqueous solution. They make it possible to determine the period and relative amplitude of oscillation, or the existence of multiple steady states, but they provide only a mixed potential when more than one redox reaction plays a major role. In oxyhalogen-containing systems, ion-selective electrodes may be employed to measure bromide, chloride or iodide concentrations. For pH oscillators, a combination glass electrode is routinely used. For reactions in which colored species are present, running the reaction in the sample compartment of a UV-visible spectrophotometer provides an attractive alternative to potentiometric measurement, particularly since modern diode array instruments afford the possibility of obtaining multiwavelength measurements and hence of following two or more species simultaneously. For nonisothermal systems, one can, of course, track the temperature.

More sophisticated techniques that have been used to monitor temporal oscillation include electron spin resonance to detect malonyl radicals in the BZ reaction[122] and to follow the cobalt-catalysed oxidation of benzaldehyde[123] and nuclear magnetic resonance to study the enolization step in the BZ reaction.[124] Magnetic resonance imaging has been used to investigate propagating fronts in the manganese-catalysed BZ reaction[125] and in the polymerization of methacrylic acid.[126] By far the most elaborate experimental methods have been employed in the beautiful studies of the Berlin group on the spatiotemporal behaviour of catalytic reactions on metal single crystals. The techniques utilised include low energy electron diffraction (LEED)[127] and photoelectron emission microscopy (PEEM).[128]

Perhaps the single most important experimental advance in nonlinear chemical dynamics was the introduction of flow reactor technology. The earliest experiments were carried out under closed system (batch) conditions, typically in beakers, cuvettes or Petri dishes. Such a configuration, while inexpensive and easy to set up, necessarily implies that key parameters, such as reactant concentrations, change throughout the course of an experiment as the system approaches equilibrium. One must be fortunate to find systems that display interesting behaviour on a time scale that is short relative to the relaxation time to the equilibrium state. Drawing on the experience of chemical engineers, investigators studying chemical oscillation in the late 1970s began to employ an open system configuration, the continuous flow stirred tank reactor (CSTR). Essentially, a CSTR, shown schematically in Fig. 12, is an elaborate beaker, equipped typically with a stirring device, a temperature jacket, one or more probes to monitor the reaction, and, most importantly, input tubes to bring fresh reactants into the system and an output tube to maintain constant volume while permitting reacted materials to leave the system. With a CSTR, a reaction can be maintained far from equilibrium indefinitely, with constant values of the control parameters—input concentrations of reactants, temperature, flow rate through the reactor. By varying pairs of control parameters, one can observe how the dynamical behaviour of the system changes and map out "dynamical phase diagrams" showing regions of the parameter space in which qualitatively different behaviour (*e.g.*, steady state, oscillatory, chaotic) occurs, or, by varying a single parameter, one can trace out hysteresis loops of the sort shown in Fig. 5. The input flow is most often regulated with a peristaltic pump, though syringe pumps provide more precise control and smoother flow. Very inexpensive (and quite reliable, though not terribly flexible) systems can be constructed using gravity-driven flows. Although one typically stirs the system at hundreds of rpm, CSTRs are only imperfectly mixed, and
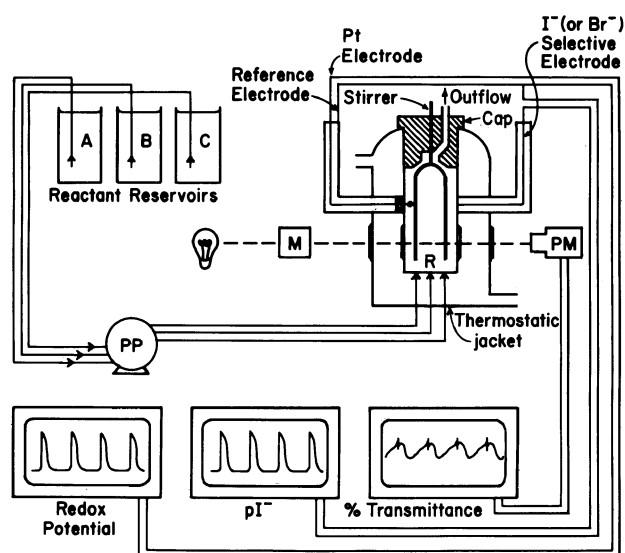

Fig. 12 Schematic drawing of a typical CSTR. PP = peristaltic pump, M = monochromator, R = reactor, PM = photomultiplier. Reproduced from ref. 20 with permission.

some reactions turn out to be quite sensitive to the rate at which they are stirred.[129]

While the CSTR is a powerful tool for studying temporal oscillation, the fact that the system is stirred renders this apparatus useless for studying spatial pattern formation. In the late 1980s several designs for continuously fed unstirred reactors (CFURs)[70,130] were introduced. In most cases, a thin disk of gel, often polyacrylamide or agarose, serves as the reaction medium. The input reagents are contained in one or more CSTRs, which allow for mixing and for the system to be maintained far from equilibrium. The reagents typically diffuse into the gel *via* a membrane or a glass capillary array, thereby minimising the effects of fluid motion within the CSTR. The high viscosity of the gel prevents convective motion, which might otherwise disturb pattern formation within the reaction zone. Other systems that have been used to study pattern formation in the BZ reaction include cation exchange beads,[131] Nafion membranes[132] and Couette reactors, in which the reaction takes place in the gap between two coaxial cylinders, one of which rotates at an adjustable speed, yielding an effective molecular diffusion coefficient proportional to the rate of rotation.[133]

The past decade has witnessed a number of exciting studies of nonlinear dynamics in electrochemical systems. Electrochemical oscillations, under either potentiostatic or galvanostatic conditions are typically several orders of magnitude faster than homogeneous chemical oscillators, making it possible to collect large quantities of data in relatively short periods of time. By introducing spatially distributed probes, one can observe spatial structures, analogous to those found in unstirred homogeneous solutions or catalytic surfaces, on working electrodes of a variety of geometries. Fronts, waves and patterns in electrochemical systems have recently been reviewed by Krischer *et al*.[134]

Mechanistic considerations

Almost from the beginning, mechanistic studies have played a key role in the development of nonlinear chemical dynamics. One might argue that it was the formulation of the FKN mechanism[16] for the BZ reaction that ultimately established the credibility of nonlinear dynamics with the majority of chemists. A persuasive case might also be made that the remarkable behaviour, both temporal and spatial, of the reactions studied by nonlinear chemical dynamicists provides the most stringent set of tests available for proposed mechanisms. Recent

advances, both on the experimental side to increase the quality and quantity of the available data, and on the computational side to make it possible to simulate models with large numbers of species, have led to the development and refinement of mechanisms for a significant number of chemical oscillators as well as to the formulation of general models for classes of oscillating reactions. Mechanistic studies of chemical oscillators, which often consist of many elementary steps, have inspired the determination of rate laws, kinetic constants and mechanisms for numerous component reactions. In addition to detailed models of individual oscillators, mechanistic studies have led to the development of several general classification schemes, which attempt to identify sets of features common to a group of chemically or dynamically related oscillators, and of new approaches to extracting mechanistic information from complex reaction systems.

Example of a specific reaction mechanism—chlorite–iodide

The BZ reaction has certainly been the most thoroughly studied from a mechanistic point of view. Although some alternatives have been proposed,[135] the original FKN mechanism[16] has stood up well over time, and most of the work of the past three decades has been devoted to filling in the details of the inorganic[136] or organic[137] portions of the FKN scheme rather than to challenging the fundamental concepts that underlie it. We shall not discuss the details of the BZ mechanism, which can be found in several review articles and collections.[2] Instead, we present here another example, which has also been quite thoroughly explored, the chlorite–iodide oscillator and related reactions.[138]

The chlorite–iodide reaction has played nearly as central a role in nonlinear chemical dynamics as the BZ system. The reaction, particularly when augmented with malonic acid, in the form of the CIMA system, displays the same wealth of spatio-temporal behaviour and also possesses several variants that enhance its versatility. Early mechanistic studies of the reaction[139,140] predate its identification with nonlinear dynamics and established its unusual character of being both autocatalytic (in the product I_2) and substrate inhibited (by the reactant I^-). In the late 1980s, several mechanisms were proposed[141,142] that successfully reproduced key aspects of the system's behaviour, notably oscillations and bistability, but none was totally successful over the entire range of experimental data. Several rate constants had not been determined experimentally and had to be fitted (or guessed). For example, the bimolecular rate constant for the reaction of HOCl and HOI was taken as zero in one model,[141b] 2×10^3 M^{-1} s^{-1} in another,[142] 5×10^5 M^{-1} s^{-1} in a third,[141c] and 2×10^8 M^{-1} s^{-1} in yet another proposed mechanism![141a] These differences were, of course, compensated by discrepancies in the values of other rate constants in the respective mechanisms.

Lengyel *et al.*[138] studied the system over a wide range of initial conditions: pH = 1–3.5, $[ClO_2^-] \leq 10^{-3}$ M, $[I^-] \leq 10^{-3}$ M, $[I^-]/[ClO_2^-]$ = 3–5. They employed multiwavelength spectrophotometry and stopped-flow techniques and carried out extensive computer simulations. Because analytically pure chlorite ion is not easily prepared, they generated ClO_2^- *in situ* from the reaction between chlorine dioxide and iodide ion. They found that the overall reaction is multiphasic, consisting of four separable parts: (a) the reaction of chlorine dioxide with iodide to generate chlorite ion; (b) the initial reaction of Cl(III) with iodide; (c) the reaction of Cl(III) with the product iodine; and (d) the disproportionation of hypoiodous and iodous acids. The overall reaction was broken down into a set of kinetically active subsystems and three rapidly established equilibria: the protonation of ClO_2^- and of HOI and the formation of I_3^-. The stoichiometry and kinetics were experimentally determined

(in some cases redetermined) or were taken from the earlier literature for the oxidation of iodine $(-1,0,+1,+3)$ by chlorine$(0,+1,+3)$, oxidation of I^- by HIO_2 and disproportionation of HOI and HIO_2. Rate constants determined for simpler systems were fixed in the more complex systems. The final mechanism, given in Table 1, consists of 13 elementary steps plus the three rapid equilibria, involving a total of 15 species. Simulations using this model fit the experimental data on both the overall reaction and all component subsystems within 1% relative accuracy. Reactions (M11)–(M13) are significant only at pH < 2.0 and high (>10^{-3} M) concentrations of $HClO_2$, or when $[Cl^-]$ is present initially, or in the $HOCl + I_2$ reaction. Otherwise they may be neglected along with Cl_2 and Cl^-.

Mechanistic classification schemes

Mechanistic analysis at something approaching the level of detail of the chlorite–iodide system has been carried out for perhaps half a dozen chemical oscillators, and partial mechanisms are available for several more. An alternative and more generally applicable approach is to identify general mechanistic features that characterise groups of oscillators. Higgins[143] examined models of biochemical oscillators from this point of view, and Tyson[144] showed by analyzing the "community matrix," which consists of the signs of the elements of the Jacobian matrix, that all processes capable of destabilising the steady state, and thus of generating oscillatory behaviour, fall into three general classes. The first attempt of this sort based on mechanisms of actual chemical oscillators was Noyes' development[145] of a comprehensive scheme for the family of bromate-based oscillators. Orbán *et al.*[29] extended this notion by suggesting that each family or subfamily of oscillators contains a minimal core from which all members may be derived.

Another approach to deriving a mechanistic understanding of a family of oscillators is to abstract from the mechanism of a particular reaction the essential dynamical features and produce a "skeleton mechanism" that is applicable to the entire family. In Table 2, we show a mechanism[146] for the bromate–sulfite–ferrocyanide reaction, a member of the family of pH oscillators.[147] The mechanism accurately describes the bistable and oscillatory behaviours of this reaction and qualitatively mimics similar phenomena in other pH oscillators. A key element is the autocatalytic production of H$^+$ *via* eqns. (B1)–(B6), which we summarise, writing A for BrO_3^-, H for H$^+$, X for SO_3^{2-}, and Y for one or more of the intermediates, such as $HBrO_2$, HOBr or Br_2, as

$$A + HX + H \longrightarrow Y \qquad (14)$$

$$HX + Y \longrightarrow 3H \qquad (15)$$

The protonation–deprotonation equilibrium, eqns. (B7) and (B8), also plays a key role and can be represented as

$$X + H \rightleftharpoons HX \qquad (16)$$

Finally, the system requires a negative feedback in order to oscillate. In the actual system, this role is played by step (B4), which removes the intermediate, and by step (B9), which consumes protons. Identifying P with Br$^-$, and B and Q with ferrocyanide and ferricyanide, respectively, we can write these two steps as

$$Y \longrightarrow P \qquad (17)$$

$$B + H \longrightarrow Q \qquad (18)$$

If step (17) is sufficiently rapid, reaction (18) may be neglected. If, conversely, step (18) is fast enough, steps (14), (15) and (17) may be merged into the single reaction

Table 1 Mechanism of the chlorite–iodide and related reactions[a]

Number	Reaction	Rate law
(M1)	$ClO_2 + I^- \longrightarrow ClO_2^- + \frac{1}{2}I_2$	$v_1 = 6 \times 10^3[ClO_2][I^-]$
(M2)	$I_2 + H_2O \rightleftharpoons HOI + I^- + H^+$	$v_{2a} = 1.98 \times 10^{-3}[I_2]/[H^+] - 3.67 \times 10^9[HOI][I^-]$
		$v_{2b} = 5.52 \times 10^{-2}[I_2] - 3.48 \times 10^9[H_2OI^+][I^-]$
(M3)	$HClO_2 + I^- + H^+ \longrightarrow HOI + HCl$	$v_3 = 7.8[HClO_2][I^-]$
(M4)	$HClO_2 + HOI \longrightarrow HIO_2 + HOCl$	$v_4 = 6.9 \times 10^7[HClO_2][HOI]$
(M5)	$HClO_2 + HIO_2 \longrightarrow IO_3^- + HOCl + H^+$	$v_5 = 1.5 \times 10^6[HClO_2][HIO_2]$
(M6)	$HOCl + I^- \longrightarrow HOI + Cl^-$	$v_6 = 4.3 \times 10^8[HOCl][I^-]$
(M7)	$HOCl + HIO_2 \longrightarrow IO_3^- + Cl^- + 2H^+$	$v_7 = 1.5 \times 10^3[HOCl][HIO_2]$
(M8)	$HIO_2 + I^- + H^+ \rightleftharpoons 2HOI$	$v_8 = 1.0 \times 10^9[HIO_2][I^-][H^+] - 22[HOI]^2$
(M9)	$2HIO_2 \longrightarrow IO_3^- + HOI + H^+$	$v_9 = 25[HIO_2]^2$
(M10)	$HIO_2 + H_2OI^+ \longrightarrow IO_3^- + I^- + 3H^+$	$v_{10} = 110[HIO_2][H_2OI^+]$
(M11)	$HOCl + Cl^- + H^+ \rightleftharpoons Cl_2 + H_2O$	$v_{11} = 2.2 \times 10^4[HOCl][Cl^-][H^+] - 22[Cl_2]$
(M12)	$Cl_2 + I_2 + 2H_2O \longrightarrow 2HOI + 2Cl^- + 2H^+$	$v_{12} = 1.5 \times 10^5[Cl_2][I_2]$
(M13)	$Cl_2 + HOI + H_2O \longrightarrow HIO_2 + 2Cl^- + 2H^+$	$v_{13} = 1.0 \times 10^6[Cl_2][HOI]$

	Rapid equilibria	
(M14)	$HClO_2 \rightleftharpoons ClO_2^- + H^+$	$K_{14} = [ClO_2^-][H^+]/[HClO_2] = 2.0 \times 10^{-2}$
(M15)	$H_2OI^+ \rightleftharpoons HOI + H^+$	$K_{15} = [HOI][H^+]/[H_2OI^+] = 3.4 \times 10^{-2}$
(M16)	$I_2 + I^- \rightleftharpoons I_3^-$	$K_{16} = [I3^-]/[I_2][I^-] = 7.4 \times 10^2$

[a] All concentrations in M, times in s.

Table 2 Mechanism for the bromate–sulfite–ferrocyanide reaction

Number	Reaction
(B1)	$BrO_3^- + HSO_3^- \longrightarrow HBrO_2 + SO_4^{2-}$
(B2)	$HBrO_2 + Br^- + H^+ \longrightarrow 2HOBr$
(B3)	$HOBr + Br^- + H^+ \longrightarrow Br_2 + H_2O$
(B4)	$Br_2 + H_2O \longrightarrow HOBr + Br^- + H$
(B5)	$2HBrO_2 \longrightarrow BrO_3^- + HOBr + H^+$
(B6)	$Br_2 + HSO_3^- + H_2O \longrightarrow 2Br^- + SO_4^{2-} + 3H^+$
(B7)	$H^+ + SO_3^{2-} \longrightarrow HSO_3^-$
(B8)	$HSO_3^- \longrightarrow H^+ + SO_3^{2-}$
(B9)	$BrO_3^- + 2Fe(CN)_6^{4-} + 3H^+ \longrightarrow HBrO_2 + 2Fe(CN)_6^{3-} + H_2O$

$$A + HX + H \longrightarrow nH \quad (n \geq 2) \qquad (19)$$
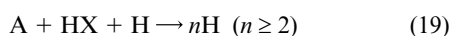
and Y eliminated as a variable. With appropriately chosen kinetic parameters, the simple model consisting of eqns. (14)–(17) or of eqns. (16) and (18) generates the clock behaviour in batch and bistability and oscillations under flow conditions of a wide variety of pH oscillators.[148]

A still more general approach is to classify oscillating reactions according to the kind of feedback that causes them to oscillate. Expanding on earlier ideas of Tyson[144] and Franck,[149] Luo and Epstein[150] proposed such a categorization based on two types of positive feedback—direct (which can be either explosive or self-limiting) and indirect autocatalysis, and three types of negative feedback—coproduct autocontrol, double autocatalysis, and flow control. An alternative classification, which utilises stoichiometric network analysis[151] to identify groups of reactions that destabilise the reaction network, has been proposed by Eiswirth et al.[152]

Approaches to analyzing complex reactions

One byproduct of efforts to construct mechanisms for chemical oscillators has been the development of new approaches to the analysis of complex, multistep reactions. The experimental capability of diode array spectrophotometers to obtain data at multiple wavelengths with a time resolution much less than the duration of a typical oscillation and the computational power of modern PCs have led to methods for treating large quantities of experimental data and extracting from them kinetic parameters. It is now possible, using sophisticated matrix manipulations along with computer simulation and fitting of differential equations,[153] to utilise data sets consisting of thousands of points to compare literally hundreds of candidate mechanisms.[154]

Other approaches, in analogy to relaxation kinetics, involve perturbation techniques. Ruoff[155] attempted to test the FKN mechanism for the BZ reaction by adding small quantities of KBr, AgNO$_3$ and HOBr and comparing the observed phase shifts of the oscillations with those predicted by the mechanism. A more general technique, developed by Hynne and Sørensen,[156] is known as *quenching*. If we think of an oscillating reaction as occurring in a space whose coordinates are the concentrations of the oscillating species, then a typical oscillation may be represented as a periodic closed curve like a circle or an ellipse, in mathematical terms a limit cycle, in that space. At the center of the limit cycle lies an unstable steady state. If one perturbs the system by adding (or subtracting) just the right amount of a reactant or intermediate at just the right phase of the oscillation, one may move the system off the limit cycle and onto (or at least into the neighbourhood of) the steady state. Although the steady state is unstable, so that the system will eventually resume oscillating, the oscillations will be quenched for a significant time. Comparing the results of a set of quenching experiments with the predictions of a model can provide a stringent test of the model.

Another perturbation method, correlation metric construction (CMC),[157] is derived from electronic circuit theory. Here one subjects a system near its steady state to random concentration changes in a set of input species. Sequences of measurements of as many concentrations as possible subsequent to the perturbation are used to construct a time-lagged correlation matrix, which measures the interspecies and time correlations within the reaction network, i.e., which species concentrations show related changes separated by a particular time interval. The resulting matrix is then converted into a set of "distances" between species. When these distances are projected onto a two-dimensional plane, a picture of the reaction network emerges. Unlike the methods described above, the CMC approach is more qualitative, but can be used to generate the reactions in a complex network rather than simply testing the quantitative success of a network consisting of a given set of reactions.
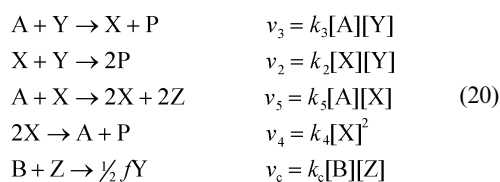
Models

As noted above, the FKN mechanism is the most widely accepted kinetic scheme for the BZ reaction. However, it involves so many chemical species and reactions that the

complete kinetic model that follows from it is analytically of very limited use. Fortunately, the structure of the FKN mechanism is so robust that it can be reduced to a much simpler model, the Oregonator (after Oregon, USA, where it was first proposed). Since its formulation by Field, Kőrös and Noyes[16] nearly thirty years ago, it has been and continues to be commonly used to interpret the dynamic behaviour of the BZ reaction, both in homogeneous and spatially dependent conditions. The reduction from the original FKN extended mechanism proceeds through the standard techniques of chemical kinetics, mainly the pseudo-steady-state and rate-limiting-step approximations.

The Oregonator model

The standard Oregonator model is commonly written in terms of five irreversible steps, whose rate constants are assumed to incorporate proton concentrations when appropriate. The sequence of basic reactions may be written as:

$$
\begin{aligned}
A + Y &\rightarrow X + P & v_3 &= k_3[A][Y] \\
X + Y &\rightarrow 2P & v_2 &= k_2[X][Y] \\
A + X &\rightarrow 2X + 2Z & v_5 &= k_5[A][X] \\
2X &\rightarrow A + P & v_4 &= k_4[X]^2 \\
B + Z &\rightarrow \tfrac{1}{2} fY & v_c &= k_c[B][Z]
\end{aligned} \tag{20}
$$

In this scheme, $A = BrO_3^-$; $B = $ organic species such as malonic acid and bromomalonic acid; $P = HOBr$; $X = HBrO_2$; $Y = Br^-$, $Z = $ oxidized form of the catalyst; and f is a stoichiometric factor that serves as an adjustable parameter. In what follows we assume that the major reactants A and B are kept at fixed concentrations and focus our analysis on the three intermediates X, Y and Z. The corresponding rate equations are:

$$
\begin{aligned}
\frac{d[X]}{dt} &= k_3[A][Y] - k_2[X][Y] + k_5[A][X] - 2k_4[X]^2 \\
\frac{d[Y]}{dt} &= -k_3[A][Y] - k_2[X][Y] + \tfrac{1}{2} f k_c[B][Z] \\
\frac{d[Z]}{dt} &= 2k_5[A][X] - k_c[B][Z]
\end{aligned} \tag{21}
$$

The analysis is greatly simplified by converting these equations to a dimensionless form. The appropriate conversion factors are:

$$
x \equiv \frac{2k_4[X]}{k_5[A]} \qquad y \equiv \frac{k_2[Y]}{k_5[A]} \qquad z \equiv \frac{k_c k_4[B][Z]}{(k_5[A])^2} \tag{22}
$$

$$
t \equiv k_c[B]T
$$

Introducing some additional dimensionless parameters, we obtain a simpler form of the kinetic equations:

$$
\begin{aligned}
\frac{dx}{dt} &= \frac{qy - xy + x(1-x)}{\varepsilon} \\
\frac{dy}{dt} &= \frac{-qy - xy + fz}{\varepsilon'} \\
\frac{dz}{dt} &= x - z
\end{aligned} \tag{23}
$$

The three dimensionless parameters remaining in eqn. (23) have typical values of $\varepsilon \approx 10^{-2}$, $\varepsilon' \approx 10^{-5}$, $q \approx 10^{-4}$. Note that the autocatalytic contribution, the genuine nonlinear term in the dynamics of the Oregonator model, is clearly identified through the term $x(1-x)$.

Even in this form, the Oregonator model appears formidable from an analytical point of view. We pursue a further reduction of the original set of equations to a form that still captures the basic nonlinear dynamic features of the BZ reaction. To this end we take advantage of the smallness of the quantities ε and ε', respectively associated with the time scales governing the evolution of $HBrO_2$ and Br^-. Since ε' is much smaller than ε, one can invoke the steady state approximation for the concentration of bromide ion to obtain $y = fz/(q + x)$. Substituting this result into eqn. (23), we end up with a pair of rate equations for the bromous acid concentration and the oxidized form of the catalyst:

$$
\begin{aligned}
\varepsilon \frac{dx}{dt} &= x(1-x) + f\frac{q-x}{q+x}z \\
\frac{dz}{dt} &= x - z
\end{aligned} \tag{24}
$$

Written in this way, the reduced Oregonator model has the typical form of an activator-inhibitor model, with x the autocatalytic (activator) species, and z the consuming species (inhibitor).

Phase-space analysis of stability: oscillating and excitable regimes

The simplest behaviour of the BZ reaction we aim at reproducing with the kinetic scheme just derived consists of temporal oscillations. Naturally, temporal oscillations emerge, rather than the "classical" monotonic approach to a steady state, as a consequence of the loss of stability of the steady state solution. Our task is thus to obtain the steady state solutions, classify them in terms of some parameter (for instance, f) and check their stability properties. Such a stability analysis can be done *a posteriori* by direct numerical integration of the differential equations. A more elegant approach invokes analytical linear stability techniques.[158] There is, however, a much more intuitive *a priori* technique based on the notion of trajectories in the phase space spanned by the set of variables of our dynamical system.[159] A curve in this space is nothing but the succession of states attained by the system as it evolves in time. We look briefly at how this tool enables us to interpret pictorially the onset of oscillations in the two-variable Oregonator model (24).

A pair of special curves easily constructed in the phase space of our system turn out to be particularly important for our discussion (Fig. 13). They are the so-called nullclines, which locate the (x, z) pairs such that $dx/dt = 0$ (x-nullcline) and $dz/dt = 0$ (z-nullcline). In the reduced Oregonator model, the z-nullcline for the inhibitor variable is a straight line with slope unity and passing through the origin. The x-nullcline for the activator species has a more complicated (inverted N) shape. The curves intersect at a single point, which corresponds to the steady state. Several distinct scenarios can be envisaged by considering the position of this crossing point relative to the nullclines. Depending on the value of the parameter f, the nullclines intersect to the right (left) of the maximum (minimum) of the x-nullcline, for low (high) values of that parameter, or, alternatively, they cross on the middle branch, for intermediate values of f. The stability of the corresponding steady states is easily determined by using the fact that the nullclines separate the phase plane into four different regions each with a different combination of the signs of the derivatives dx/dt and dz/dt (Fig. 13).

By simply following trajectories starting from arbitrary points in the phase space, we convince ourselves that whenever the steady states are located either on the left or on the right branch, they are stable, whereas any steady state located on the middle branch is unstable. In this last situation (Fig. 14a), if one starts with an arbitrary initial condition, *e.g.*, below the x-nullcline, the system jumps, nearly horizontally, $dx/dt \gg 0$,
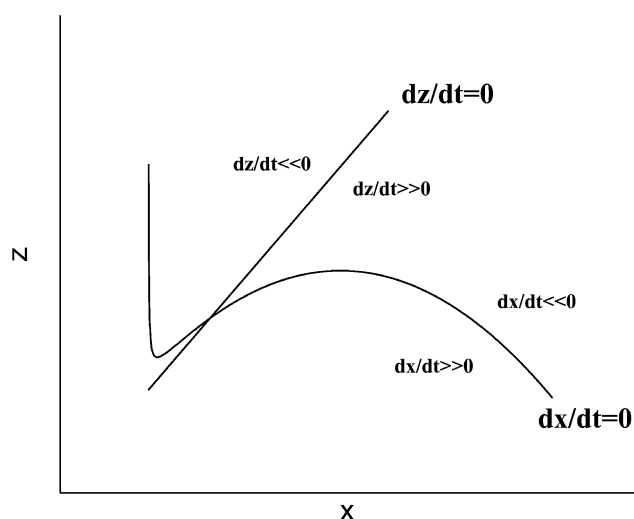
Fig. 13 Phase space representation of the reduced Oregonator model showing the *x*- and *z*-nullclines. Parameter values are: $\varepsilon = 0.03$, $q = 0.015$ and $f = 1.0$.

to the right branch and then moves upward, ($dz/dt > 0$), approaching the maximum of the *x*-nullcline. At this point dz/dt is still positive, so the trajectory has to leave the nullcline, this time jumping backwards toward the left branch. On crossing this branch, dz/dt changes sign, so the trajectory goes downward and approaches the minimum. Since at this point dz/dt is still negative, the trajectory is forced again to leave the nullcline and this time is projected toward the right branch to repeat the cycle forever. There is thus no possibility for the system to reach its steady state, but instead it gets trapped in a "limit cycle" trajectory, a signature of its oscillatory behaviour.
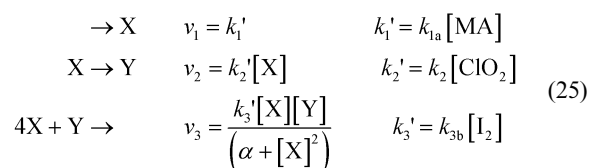
The phase-space analysis of excitability, rather than of oscillatory behaviour, proceeds similarly (Fig. 14b). Assume now that the intersection point is located on the left branch, but very close to the minimum of the *x*-nullcline. If, starting from rest, the system is slightly (subcritically) perturbed in such a way that it remains to the left of the middle branch, a monotonic relaxation back to the steady state will take place. If it is instead perturbed strongly enough (supercritically), so that it crosses the middle branch, then the dynamics will take the system through a large excursion around the phase plane before return-

ing to the rest state. Note in this case that the important notion of refractoriness is easily understood within our phase space representation. The system is effectively insensitive to any further excitation during the slow evolution along the right branch of the *x*-nullcline and as it begins to descend along the left branch. It is only when it approaches the rest state that the middle branch is again reachable and the system regains its excitability.

As mentioned above and when considering unstirred reactors, oscillatory or excitable conditions can give rise to striking spatially extended phenomena of wave propagation. True waves, either isolated, in the form of single pulses, or collectively organized as wave trains (target patterns), propagate based on a reaction–diffusion mechanism. The simplest situation occurs under excitable conditions, where the role of the perturbative excitation at any point of the extended system can be played by a diffusional flow from neighboring elements of the medium. Naturally in this case, the model used so far and appropriate to zero-dimensional (point or well-stirred) systems, has to be extended to include diffusion.

Modeling Turing-like patterns

Up to now in this section we have analyzed typical phenomena occurring in the BZ reaction that can be easily accounted for, at least qualitatively, with the standard Oregonator model, or even more advantageously, in terms of its reduced two-variable, form (24). We now consider the modeling of stationary Turing patterns, which do not arise in the ordinary BZ reaction, but do occur in the CIMA system. The CIMA reaction also admits a convenient description in terms of a two-variable activator–inhibitor model [71]

$$
\begin{aligned}
&\rightarrow X & v_1 &= k_1' & k_1' &= k_{1a}[MA] \\
&X \rightarrow Y & v_2 &= k_2'[X] & k_2' &= k_2[ClO_2] \\
&4X + Y \rightarrow & v_3 &= \frac{k_3'[X][Y]}{(\alpha + [X]^2)} & k_3' &= k_{3b}[I_2]
\end{aligned} \tag{25}
$$

where $X = I^-$ stands for the activator, $Y = ClO_2^-$ is the inhibitor species and α denotes a phenomenological parameter. The resulting rate laws can be nondimensionalized (omitting the details) into the form
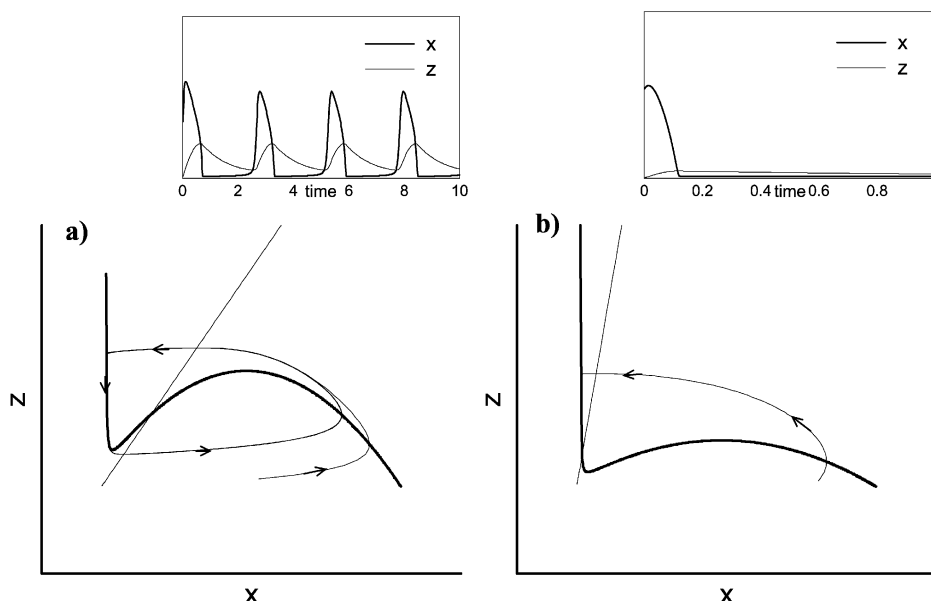
Fig. 14 Phase space representation of the reduced Oregonator model: a) Oscillatory regime; b) Excitable regime. Parameter values ε and q as in Fig. 13, $f = 1.0$ (a) and $f = 10$ (b).

$$\frac{du}{dt} = a - u - \frac{4uv}{\left(1 + u^2\right)}$$

$$\frac{dv}{dt} = b\left[u - \frac{uv}{\left(1 + u^2\right)}\right] \qquad (26)$$

There are two key features of Turing-like structures that must be reproduced by any model aimed at their study. First they must arise through instabilities of steady states that are stable to homogeneous perturbation. Second, the patterned state must have an intrinsic wavelength that is determined solely by the kinetic and diffusion parameters, but is independent of the size of the system (provided this dimension is larger than the wavelength).

The onset of Turing patterns can be described mathematically in a straightforward way. To illustrate this procedure we look at a one-dimensional generic activator–inhibitor model of the sort we have written above for the CIMA reaction, expanded to include diffusion terms as

$$\frac{\partial u}{\partial t} = f\left(u, v\right) + \frac{\partial^2 u}{\partial x^2}$$

$$\frac{\partial v}{\partial t} = g\left(u, v\right) + D\frac{\partial^2 v}{\partial x^2} \qquad (27)$$

Note that for convenience we have defined D to be the ratio of diffusivities of the two species, since one of the diffusion coefficients, in this case that corresponding to the activator variable, can be used to nondimensionalize the spatial scale.

We assume that the system has a homogeneous steady state (u_{ss}, v_{ss}), such that $f(u_{ss}, v_{ss}) = g(u_{ss}, v_{ss}) = 0$. A linear stability analysis of such a solution in the absence of diffusion, $i.e.$, for homogeneous perturbations, is easily formulated in terms of the Jacobian matrix constructed from the kinetic terms. We write it as, $A|_{(u_{ss}, v_{ss})}$ where the notation reminds us that the Jacobian is evaluated at the reference steady state solution. Its components are the partial derivatives of the kinetic functions

$$a_{11} = \frac{\partial f}{\partial u} \equiv f_u \qquad a_{12} \equiv f_v \qquad a_{21} \equiv g_u \qquad a_{22} \equiv g_v \qquad (28)$$

The eigenvalues of the linear stability analysis are directly obtained as

$$\lambda_{1,2} = \frac{Tr\left(A\right) \pm \left[Tr\left(A\right)^2 - 4|A|\right]^{1/2}}{2} \qquad (29)$$

in terms of the trace $Tr(A) = f_u + g_v$, and the determinant, $|A| = f_u g_v - f_v g_u$, of the Jacobian. Stability is guaranteed if $Tr(A) < 0$ and $|A| > 0$.

Now let us consider stability with respect to inhomogeneous perturbations of the form $(u, v) \propto (u_0, v_0)e^{\lambda \tau \pm ikx}$. The Jacobian matrix now incorporates the diffusion terms, and the corresponding eigenvalues read

$$\lambda_{1,2} = \frac{\left[Tr\left(A\right) - k^2\left(D + 1\right) \pm \left[\left[Tr\left(A\right) - k^2\left(D + 1\right)\right]^2 - 4h\left(k^2\right)\right]\right]^{1/2}}{2} \qquad (30)$$

with $h(k^2) \equiv Dk^4 - (Df_u + g_v)k^2 + |A|$. The only possibility for the steady state to be unstable is that $h(k^2) < 0$ for some nonzero value of k at which $Re[\lambda(k)] > 0$. As a function of k^2, $h(k^2)$ has a minimum, and, since $|A| > 0$, $(Df_u + g_v)$ must be positive. On the other hand, recall that $Tr(A) = f_u + g_v$ is negative, so we must have $D \neq 1$ as a necessary condition for a Turing-like instability.

Indeed, f_u and g_v must be of opposite sign. For convenience, suppose that $f_u > 0$ and $g_v < 0$, in accordance with the activator–inhibitor classification in our two-species model. Then $D > 1$, $i.e.$, the inhibitor diffuses faster than the activator. This important restriction is characteristic of the Turing instability.

Although the last inequality on the ratio of diffusion coefficients is a necessary condition, it is not sufficient for instability ($i.e.$, to ensure that $h(k^2) < 0$). More precisely, we require that the minimum of h be negative, which requires that

$$(Df_u + g_v)^2 > 4D|A| \qquad (31)$$

At the bifurcation, i.e. when $h_{min} = 0$, we can obtain a critical value for D, as well as the critical value of the wavenumber at the onset of the instability

$$D_c^2 f_u^2 + 2\left(2f_v g_u - f_u g_v\right)D_c + g_v^2 = 0$$

$$k_c^2 = \frac{D_c f_u + g_v}{2D_c} = \left[\frac{f_u g_v - f_v g_u}{D_c}\right]^{1/2} \qquad (32)$$

This summarizes our mathematical description of the Turing instability.

Future prospects

Nonlinear chemical dynamics has grown rapidly, perhaps exponentially, during the past three decades. While we hesitate to predict where such a vital field will move in the future, it seems appropriate to suggest a few areas that are likely to grow in prominence in the coming years. Increasingly, the complex chemical reactions studied by nonlinear dynamicists are being coupled to other phenomena that have generally been considered to belong more to the domains of physics or biology. The effects of linking "exotic" chemical reactions to hydrodynamics, surface tension, fluid flows and mechanical forces are likely to become significant areas of research. We expect the insights of nonlinear chemical dynamics to be applied to systems much larger and much smaller than the beakers, Petri dishes and laboratory scale reactors that have played the major roles to date. The oceans and the atmosphere are two realms in which nonlinear chemical dynamics has only begun to have an impact, though its relevance is already clear.

Going down from the typical laboratory scale, a particularly interesting context is that of nonequilibrium structures in soft-condensed systems.[160] All the chemical phenomena reported so far in this article refer to "dilute"systems, where physical interactions between reacting molecules can be neglected. But nonequilibrium structures can also appear in condensed systems of particles with weak attractive interactions (liquid crystals, lipid membranes or vesicles, Langmuir or Langmuir–Blodgett films, thin liquid films on solid surfaces and adsorbate layers in metals). In particular, promising reports have already appeared of wave propagation phenomena in Langmuir monolayers of amphiphilic photoisomerization compounds.[161] On the micro-, even the nano-scale, we point out that the water droplets in which the BZ reaction occurs in the microemulsion system in Fig. 8 have volumes of about 10^{-22} L. It has recently been reported that the BZ oscillator can be used to direct the periodic, stepwise self-assembly of acrylonitrile-derivatised gold nanocrystals.[162]

Thus far, nonlinear chemical dynamics has been a relatively "pure" science, with few applications of practical importance. We expect that situation to change as studies of catalysis,[127] the use of oscillating reactions in gels to create devices for drug delivery,[163] and the production of new materials via frontal polymerization[164] along with other, so far unforeseen, applications evolve. Future progress will almost certainly involve working with and developing new approaches to

"dirtier"systems—heterogeneous materials, media that change in size and shape, highly coupled configurations. Continued development of approaches that enable investigators to control and design dynamical behaviour, both in time and in space, is likely to play a key role, aided by further progress in experimental methods and computational power. Finally, we expect nonlinear chemical dynamics to remain what it has always been, a vibrant, interdisciplinary, international field where theory and experiment are inextricably linked.

Acknowledgements

References and notes

1 For some recent examples, see G. W. Coates, *J. Chem. Soc., Dalton Trans.*, 2002, 467–475; D. L. Rieger, R. F. Semeniuc and M. D. Smith, *J. Chem. Soc., Dalton Trans.*, 2002, 476–477; D. Sun, R. Cao, J. Weng, M. Hong and Y. Liang, *J. Chem. Soc., Dalton Trans.*, 2002, 291–292; R. Prabaharan, N. C. Fletcher and M. Nieuwenhuyzen, *J. Chem. Soc., Dalton Trans.*, 2002, 602–608.

2 I. R. Epstein and J. A. Pojman, *Introduction to Nonlinear Chemical Dynamics. Oscillations, Waves, Patterns and Chaos*, Oxford University Press, New York, 1998; *Chemical Waves and Patterns*, R. Kapral and K. Showalter, eds., Kluwer, Dordrecht, 1995; P. Gray and S. K. Scott, *Chemical Oscillations and Instabilities: Nonlinear Chemical Kinetics*, Clarendon, Oxford, 1995; *Oscillations and Traveling Waves in Chemical Systems*, R. J. Field and M. Burger, eds., Wiley, New York, 1985.

3 S. H. Strogatz, *Nonlinear Dynamics and Chaos with Applications to Physics, Biology, Chemistry and Engineering*, Addison-Wesley, Reading, MA, 1994.

4 M. Eigen, *Pure Appl. Chem.*, 1963, **6**, 97–115; C. Bernasconi, *Relaxation Kinetics*, Academic Press, New York, 1976.

5 A. T. Fechner, *Schweigg. J.*, 1828, **53**, 61–76.

6 W. C. Bray, *J. Am. Chem. Soc.*, 1921, **43**, 1262–1267.

7 See, *e.g.* F. Rice and O. Reiff, *J. Phys. Chem.*, 1927, **31**, 1352–1356; M. Peard and C. Cullis, *Trans. Faraday Soc.*, 1951, **47**, 616–630.

8 B. P. Belousov, *Sbornik Referator po Radiatsioni Medizin (conference proceedings)*, 1958, p. 145.

9 A. M. Zhabotinsky, *Biofizika*, 1964, **9**, 306–311.

10 C. Vidal, J. C. Roux and A. Rossi, *J. Am. Chem. Soc.*, 1980, **102**, 5707–5712.

11 (phen) = 1,10-Phenanthroline; (bipy) = 2,2′-bipyridine.

12 A. N. Zaikin and A. M. Zhabotinsky, *Nature*, 1970, **225**, 535–537.

13 F. Siegert and C. Weijer, *J. Cell. Sci.*, 1989, **93**, 325–335.

14 J. Lechleiter, S. Girard, E. Peralta and D. Clapham, *Science*, 1991, **252**, 123–126.

15 L. Kuhnert, K. I. Agladze and V. I. Krinsky, *Nature*, 1989, **337**, 244–245.

16 R. J. Field, E. Körös and R. M. Noyes, *J. Am. Chem. Soc.*, 1972, **94**, 8649–8664.

17 D. Edelson, R. J. Field and R. M. Noyes, *Int. J. Chem. Kinet.*, 1975, **7**, 417–432.

18 P. Glansdorff and I. Prigogine, *Thermodynamics of Structure, Stability and Fluctuations*, Wiley-Interscience, New York, 1971.

19 J. Boissonade and P. De Kepper, *J. Phys. Chem.*, 1980, **84**, 501–506.

20 I. R. Epstein, *J. Chem. Educ.*, 1989, **66**, 191–195.

21 P. De Kepper, I. R. Epstein and K. Kustin, *J. Am. Chem. Soc.*, 1981, **103**, 6121–6127.

22 P. De Kepper, K. Kustin and I. R. Epstein, *J. Am. Chem. Soc.*, 1981, **103**, 2133–2134.

23 I. R. Epstein and K. Kustin, *Struct. Bonding (Berlin)*, 1984, **56**, 1–33.

24 M. Orbán and I. R. Epstein, *J. Am. Chem. Soc.*, 1985, **107**, 2302–2305; G.A. Frerichs, T.M. Mlnarik, R.J. Grun and R.C. Thompson, *J. Phys. Chem. A*, 2001, **105**, 829–837.

25 K. Kurin-Csörgei, M. Orbán, A. M. Zhabotinsky and I. R. Epstein, *Faraday Discuss.*, 2001, **120**, 11–19.

26 J. H. Jensen, *J. Am. Chem. Soc.*, 1983, **105**, 2639–2641.

27 X. He, K. Kustin, I. Nagypál and G. Peintler, *Inorg. Chem.*, 1994, **33**, 2077–2078.

28 C. J. Doona, K. Kustin, M. Orbán and I. R. Epstein, *J. Am. Chem. Soc.*, 1991, **113**, 7484–7489.

29 M. Orbán, P. De Kepper and I. R. Epstein, *J. Am. Chem. Soc.*, 1982, **104**, 2657–2658.

30 A. Hanna, A. Saul and K. Showalter, *J. Am. Chem. Soc.*, 1982, **104**, 3838–3834.

31 S. Dushman, *J. Phys. Chem.*, 1904, **8**, 453–482.

32 J. R. Roebuck, *J. Phys. Chem.*, 1902, **6**, 365–398.

33 M. Alamgir, P. De Kepper, M. Orbán and I. R. Epstein, *J. Am. Chem. Soc.*, 1983, **105**, 2641–2643.

34 M. Alamgir and I. R. Epstein, *J. Am. Chem. Soc.*, 1983, **105**, 2500–2502.

35 M. Orbán, C. Dateo, P. De Kepper and I. R. Epstein, *J. Am. Chem. Soc.*, 1982, **104**, 5911–5918.

36 J. Maselko and I. R. Epstein, *J. Phys. Chem.*, 1984, **88**, 5305–5308.

37 P. Blanchedeau, J. Boissonade and P. De Kepper, *Physica D (Amsterdam)*, 2000, **147**, 283–299.

38 M. Alamgir and I. R. Epstein, *J. Phys. Chem.*, 1984, **88**, 2848–2851.

39 C. E. Dateo, M. Orbán, P. De Kepper and I. R. Epstein, *J. Am. Chem. Soc.*, 1982, **104**, 504–509.

40 M. F. Crowley and I. R. Epstein, *J. Phys. Chem.*, 1989, **93**, 2496–2502.

41 J.-P. Laplante and T. Erneux, *J. Phys. Chem.*, 1992, **96**, 4931–4934.

42 J.-P. Laplante, M. Pemberton, A. Hjelmfelt and J. Ross, *J. Phys. Chem.*, 1995, **99**, 10063–10065.

43 J. Gleick, *Chaos: Making a New Science*, Viking, New York, 1987.

44 S. K. Scott, *Chemical Chaos*, Oxford University Press, Oxford, 1993.

45 M. J. Feigenbaum, *J. Stat. Phys.*, 1978, **19**, 25–52.

46 M. Orbán and I. R. Epstein, *J. Phys. Chem.*, 1982, **86**, 3907–3910.

47 J. L. Hudson, M. Hart and J. Marinko, *J. Chem. Phys.*, 1979, **71**, 1601–1606; J. S. Turner, J. C. Roux, W. D. McCormick and H. L. Swinney, *Phys. Lett.*, 1981, **85**, 9–12.

48 G. Rábai, *J. Phys. Chem. A*, 1997, **101**, 7085–7089.

49 E. Wasserman, *Chem. Eng. News*, 1991, **69(3)**, 25.

50 B. R. Johnson and S. K. Scott, *J. Chem. Soc., Faraday Trans.*, 1990, **86**, 3701–3705.

51 M. R. Bassett and J. L. Hudson, *J. Phys. Chem.*, 1988, **92**, 6963–6966; F. N. Albahadily and M. Schell, *J. Chem. Phys.*, 1988, **88**, 4312–4319.

52 E. Ott, C. Grebogi and J. A. Yorke, *Phys. Rev. Lett.*, 1990, **64**, 1196–1199.

53 V. Petrov, V. Gáspár, J. Masere and K. Showalter, *Nature*, 1993, **381**, 240–243.

54 M. L. Davies, P. A. Hawford-Maw, J. Hill, M. R. Tinsley, B. R. Johnson, S. K. Scott, I. Z. Kiss and V. Gáspár, *J. Phys. Chem. A*, 2000, **104**, 9944–9952.

55 E. M. Bollt and M. Dolnik, *Phys. Rev. E*, 1997, **55**, 6404–6413.

56 S. K. Scott and K. Showalter, *J. Phys. Chem.*, 1992, **96**, 8702–8711.

57 I. P. Nagy, A. Kerestessy and J. A. Pojman, *J. Phys. Chem.*, 1995, **99**, 5385–5388.

58 R. J. Field and R. M. Noyes, *J. Am. Chem. Soc.*, 1974, **96**, 2001–2006.

59 G. Bazsa and I. R. Epstein, *J. Phys. Chem.*, 1985, **89**, 3050–3053.

60 L. Szirovicza, I. Nagypál and E. Boga, *J. Am. Chem. Soc.*, 1989, **111**, 2842–2845.

61 A. T. Winfree, *The Geometry of Biological Time*, Springer, Berlin, 1980.

62 M. Bär, N. Gottschalk, M. Eiswirth and G. Ertl, *J. Chem. Phys.*, 1994, **100**, 1202–1214.

63 M. Eiswirth and G. Ertl, in *Chemical Waves and Patterns*, R. Kapral and K. Showalter, eds., Kluwer, Dordrecht, 1995, pp. 444–483; J. Verdasca, P. Borckmans and G. Dewel, *Phys. Chem. Chem. Phys.*, 2002, **4**, 1355–1366.

64 A. Winfree, *Science*, 1972, **175**, 634–635.

65 A. T. Winfree and S.H. Strogatz, *Physica*, 1984, **13D**, 221–233.

66 J. P. Keener and J. Sneyd, *Mathematical Physiology*, Springer-Verlag, New York, 1998; L. Glass and M. C. Mackey, *From Clocks to Chaos: the Rhythms of Life*, Princeton University Press, Princeton, NJ, 1988.

67 A.V. Holden, *Nature*, 1998, **392**, 20–21.

68 A. M. Turing, *Philos. Trans. R. Soc. London, B*, 1952, **237**, 37–72.

69 J. D. Murray, *Mathematical Biology*, Springer, Berlin, 1989.

70 V. Castets, E. Dulos, J. Boissonade and P. De Kepper, *Phys. Rev. Lett.*, 1990, **64**, 2953–2956.

71 I. Lengyel and I. R. Epstein, *Science*, 1991, **251**, 650–652.

72 I. Lengyel and I. R. Epstein, *Proc. Natl. Acad. Sci. USA*, 1992, **89**, 3977–3979.

73 Q. Ouyang and H. L. Swinney, *Nature*, 1991, **352**, 610–612.

74 A. De Wit, G. Dewel, P. Borckmans and D. Walgraef, *Physica D (Amsterdam)*, 1992, **61**, 289–296.

75 V. K. Vanag and I. R. Epstein, *Phys. Rev. Lett.*, 2001, **87**, 228301.

76 V. K. Vanag and I. R. Epstein, *Science*, 2001, **294**, 835–837.

77 V. K. Vanag and I. R. Epstein, *Phys. Rev. Lett.*, 2002, **88**, 88303.

78 V. K. Vanag and I. R. Epstein, *Phys. Rev. Lett.*, 2003, **90**, 098301.

79 I. Nagypál, G. Bazsa and I. R. Epstein, *J. Am. Chem. Soc.*, 1986, **108**, 3635–3640.

80 J. A. Pojman and I. R. Epstein, *J. Phys Chem.*, 1990, **94**, 4966–4972; J.A. Pojman, I. P. Nagy and I. R. Epstein, *J. Phys. Chem.*, 1991, **95**, 1306–1311.

81 All known front-propagating reactions are exothermic.

82 M. L. Kagan, S. Peleg, E. Meisels and D. Avnir, in *Modelling of Patterns in Space and Time*, Lecture Notes in Biomathematics, W. Jäger and J. D. Murray, eds., vol. 55, Springer, Berlin, 1984, pp. 146–156.

83 L. Adamcíková and P. Ševcík, *J. Chem. Educ.*, 1998, **75**, 1580.

84 A. J. Pons, F. Sagués, M. A. Bees and P.G. Sorensen, *J. Phys. Chem.*, 2000, **104**, 2251–2259.

85 M. A. Bees, A. J. Pons, P. G. Sorensen and F. Sagués, *J. Chem. Phys.*, 2001, **114**, 1932–1943.

86 M. Wiedemann, V. M. Fernandes-de Lima and W. Hanke, *Phys. Chem. Chem. Phys.*, 2002, **4**, 1370–1373.

87 M. Pinsky, *The EMF Book: What You Should Know about Electromagnetic Fields, Electromagnetic Radiation, Your Health*, Warner, New York, 1995.

88 K. J. Lohmann, *Sci. Amer.*, 1992, **266**, 100–107.

89 H. Ševcíková and M. Marek, *Physica D (Amsterdam)*, 1983, **9**, 140–156; H. Ševcíková and M. Marek, *Physica D (Amsterdam)*, 1986, **21**, 61–77.

90 A. F. Münster, P. Hasal, D. Snita and M. Marek, *Phys. Rev. E*, 1995, **50**, 546–550; P. Hasal, V. Nevorl, I. Schreiber, H. Ševcíková, D. Snita and M. Marek, in *Nonlinear Dynamics, Chaotic and Complex Systems*, E. Infeld, R. Zelazny and A. Galkowski, eds., Cambridge University Press, Cambridge, 1997, pp. 72–98.

91 O. Steinbock, J. Schütze and S.C. Müller, *Phys. Rev. Lett.*, 1992, **68**, 248–251; K. I. Agaldze and P. De Kepper, *J. Phys. Chem.*, 1992, **96**, 5239–5242.

92 V. Perez-Muñuzuri, R. Aliev, B. Vasiev, V. Perez-Villar and V. I. Krinsky, *Nature*, 1991, **353**, 740–742.

93 J. Schütze, O. Steinbock and S. C. Müller, *Nature*, 1992, **356**, 45–47.

94 E. Boga, S. Kádár, G. Peintler and I. Nagypál, *Nature*, 1990, **347**, 749–751 see also ref. 26.

95 There have, however, been some studies of temperature effects on homogeneous oscillators; see, *e.g.* E. Kumpinsky and I. R. Epstein, *J. Phys. Chem.*, 1985, **89**, 688–692.

96 K. F. Jensen and W. H. Ray, *Chem. Eng. Sci.*, 1980, **35**, 2436–2457; B. C. Sales, J. E. Turner and M. B. Maple, *Surf. Sci.*, 1982, **114**, 381–394.

97 C. Wandrey and A. Renken, *Chem. Ing. Tech.*, 1973, **45**, 845–860.

98 M. Vinson, S. Mironov, S. Mulvey and A. Pertsov, *Nature*, 1997, **386**, 477–480.

99 A. S. Mikhailov, *Foundations of Synergetics I: Distributed Active Systems*, Springer Series in Synergetics, vol. 51, Springer-Verlag, Berlin, 1994.

100 E. C. Zimmerman and J. Ross, *J. Chem. Phys.*, 1984, **80**, 720–729.

101 The introduction of a delay can vastly enhance the repertoire of behaviour of even the simplest chemical system. See, *e.g.* I. R. Epstein, *Int. Rev. Phys. Chem.*, 1992, **11**, 135–160.

102 E. C. Zimmerman, M. Schell and J. Ross, *J. Chem. Phys.*, 1984, **81**, 1327–1336.

103 A. Kaminaga and I. Hanazaki, *J. Phys. Chem. A*, 1998, **102**, 3307–3314.

104 V. Petrov, Q. Ouyang, G. Li and H. L. Swinney, *J. Phys. Chem.*, 1996, **100**, 18992–18996.

105 A. P. Muñuzuri, V. Pérez-Villar and M. Markus, *Phys. Rev. Lett.*, 1997, **79**, 1941–1944.

106 M. Markus, Z. Nagy-Ungvarai and B. Hess, *Science*, 1992, **257**, 225–227.

107 O. Steinbock, V. Zykov and S. C. Müller, *Nature*, 1993, **366**, 322–324.

108 S. Grill, V. S. Zykov and S. C. Müller, *J. Phys. Chem.*, 1996, **100**, 19082–19088; A. Karma and V. S. Zykov, *Phys. Rev. Lett.*, 1999, **83**, 2453–2456.

109 T. Sakurai, E. Mihaliuk, F. Chirilla and K. Showalter, *Science*, 2002, **296**, 2009–2012.

110 S. Alonso, F. Sagués and A. S. Mikhailov, Taming Winfree turbulence of scroll waves in excitable media, *Science*, Mar. 7 2003.

111 V. Petrov, Q. Ouyang and H. L. Swinney, *Nature*, 1997, **388**, 655–657; A. L. Lin, M. Bertram, K. Martinez, H. L. Swinney, A. Ardelea and G. F. Carey, *Phys. Rev. Lett.*, 2000, **84**, 4240–4243.

112 V. K. Vanag, L. Yang, M. Dolnik, A. M. Zhabotinsky and I. R. Epstein, *Nature*, 2000, **406**, 389–391; V. K. Vanag, A. M. Zhabotinsky and I. R. Epstein, *Phys. Rev. Lett.*, 2001, **86**, 552–555.

113 S. Kádár, J. Wang and K. Showalter, *Nature*, 1998, **391**, 770–772.

114 S. Alonso, I. Sendiña-Nadal, V. Pérez-Muñuzuri, J. M. Sancho and F. Sagués, *Phys. Rev. Lett.*, 2001, **87**, 78302; S. Alonso, F. Sagués and J. M. Sancho, *Phys. Rev. E*, 2002, **65**, 66107.

115 I. Sendiña-Nadal, A. P. Muñuzuri, D. Vives, V. Pérez-Muñuzuri, J. Casademunt, L. Ramírez-Piscina, J. M. Sancho and F. Sagués, *Phys. Rev. Lett.*, 1998, **80**, 5437–5440; I. Sendiña-Nadal, D. Roncaglia, D. Vives, V. Pérez-Muñuzuri, M. Gómez-Gesteira, V. Pérez-Villar, J. Echave, J. Casademunt, L. Ramírez-Piscina and F. Sagués, *Phys. Rev. E*, 1998, **58**, R1183–R1186.

116 I. Sendiña-Nadal, S. Alonso, V. Pérez-Muñuzuri, M. Gómez-Gesteira, V. Pérez-Villar, L. Ramírez-Piscina, J. Casademunt, J. M. Sancho and F. Sagués, *Phys. Rev. Lett.*, 2000, **84**, 2734–2737; S. Alonso and F. Sagués, *Phys. Rev. E*, 2001, **63**, 46205.

117 V. Pérez-Muñuzuri, F. Sagués and J. M. Sancho, *Phys. Rev. E*, 2000, **62**, 94–99.

118 P. De Kepper, J. Boissonade and I. R. Epstein, *J. Phys. Chem.*, 1990, **94**, 6525–6536.

119 A. P. Muñuzuri, M. Dolnik, A. M. Zhabotinsky and I. R. Epstein, *J. Am. Chem. Soc.*, 1999, **121**, 8065–8069; A. K. Horváth, M. Dolnik, A. M. Zhabotinsky and I. R. Epstein, *J. Phys. Chem. A*, 2000, **104**, 5766–5769.

120 A. K. Horvath, M. Dolnik, A. Muñuzuri, A. M. Zhabotinsky and I. R. Epstein, *Phys. Rev. Lett.*, 1999, **83**, 2950–2952.

121 M. Dolnik, I. Berenstein, A. M. Zhabotinsky and I. R. Epstein, *Phys. Rev. Lett.*, 2001, **87**, 238301; I. Berenstein, M. Dolnik, A. M. Zhabotinsky and I. R. Epstein, Spatial Periodic Perturbation of Turing Pattern Development Using a Striped Mask, *J. Phys. Chem.*, submitted.

122 B. Venkataraman and P. G. Sørensen, *J. Phys. Chem.*, 1991, **95**, 5707–5712.

123 M. G. Roelofs and J. H. Jensen, *J. Phys. Chem.*, 1987, **91**, 3380–3382.

124 E. W. Hansen and P. Ruoff, *J. Phys. Chem.*, 1989, **93**, 2696–2704.

125 A. Tzalmona, R. L. Armstrong, M. Menzinger, A. Cross and C. Lemaire, *Chem. Phys. Lett.*, 1990, **174**, 199–202.

126 B. J. Balcom, T. A. Carpenter and L. D. Hall, *Macromolecules*, 1992, **25**, 6818–6823.

127 G. Ertl, *Science*, 1991, **254**, 1750–1755.

128 H. H. Rotermund, *J. Electron Spectrosc.*, 1999, **99**, 41–54.

129 J. C. Roux, J. Boissonade and P. De Kepper, *Phys. Lett.*, 1983, **97A**, 168–170.

130 W. Y. Tam, W. Horsthemke, Z. Noszticzius and H. L. Swinney, *J. Chem. Phys.*, 1988, **88**, 3395–3396.

131 J. Maselko, J. S. Reckley and K. Showalter, *J. Phys. Chem.*, 1989, **93**, 2774–2780.

132 D. Winston, M. Arora, J. Maselko, V. Gáspár and K. Showalter, *Nature*, 1991, **351**, 132–135.

133 Q. Ouyang, V. Castets, J. Boissonade, J. C. Roux, P. De Kepper and H. L. Swinney, *J. Chem. Phys.*, 1991, **95**, 351–360.

134 K. Krischer, N. Mazouz and P. Grauel, *Angew. Chem., Int. Ed.*, 2001, **40**, 850–869.

135 Z. Noszticzius, H. Farkas and Z. A. Schelly, *J. Chem. Phys.*, 1984, **80**, 6062–6070.

136 R. J. Field and H.-D. Försterling, *J. Phys. Chem.*, 1986, **90**, 5400–5407; H.-D. Försterling, L. Stuk, A. Barr and W. D. McCormick, *J. Phys. Chem.*, 1993, **97**, 2623–2627.

137 Y. Gao, H.-D. Försterling, Z. Noszticzius and B. Meyer, *J. Phys. Chem.*, 1994, **98**, 8377–8380; J. Oslonovitch, H.-D. Försterling, M. Wittmann and Z. Noszticzius, *J. Phys. Chem. A*, 1998, **102**, 922–927; L. Hegedus, H.-D. Försterling, M. Wittmann and Z. Noszticzius, *J. Phys. Chem. A*, 2000, **104**, 9914–9920.

138 I. Lengyel, J. Li, K. Kustin and I. R. Epstein, *J. Am. Chem. Soc.*, 1996, **118**, 3708–3719.

139 D. M. Kern and C. H. Kim, *J. Am. Chem. Soc.*, 1965, **87**, 5309–5313.

140 J. De Meeus and J. Sigalla, *J. Chim. Phys.*, 1966, **63**, 453–459.

141 (*a*) I. R. Epstein and K. Kustin, *J. Phys. Chem.*, 1985, **89**, 2275–2282; (*b*) O. Citri and I. R. Epstein, *J. Phys. Chem.*, 1987, **91**, 6034–6040; (*c*) O. Citri and I. R. Epstein, *J. Phys. Chem.*, 1988, **92**, 1865–1871.

142 G. Rábai and M. T. Beck, *Inorg. Chem.*, 1987, **26**, 1195–1199.

143 J. Higgins, *Ind. Eng. Chem.*, 1967, **59**, 18–62.

144 J. Tyson, *J. Chem. Phys.*, 1973, **58**, 3919–3930.

145 R. M. Noyes, *J. Am. Chem. Soc.*, 1980, **102**, 4644–4649.

146 E. C. Edblom, Y. Luo, M. Orbán, K. Kustin and I. R. Epstein, *J. Phys. Chem.*, 1989, **93**, 2722–2727; see G. Rabai, A. Kaminaga and I. Hanazaki, *J. Phys. Chem.*, 1996, **100**, 16441–16442 for a critique of this mechanism.

147 G. Rábai, M. Orbán and I. R. Epstein, *Acc. Chem. Res.*, 1990, **23**, 258–263.

148 Y. Luo and I. R. Epstein, *J. Am. Chem. Soc.*, 1991, **113**, 1518–1522.

149 U. F. Franck, in *Temporal Order*, L. Rensing, N. Jaeger, eds., Springer, Berlin, 1985, pp. 2–12.
150 Y. Luo and I. R. Epstein, *Adv. Chem. Phys.*, 1990, **79**, 269–299.
151 B. L. Clarke, *Adv. Chem. Phys.*, 1980, **43**, 1–215.
152 M. Eiswirth, A. Freund and J. Ross, *Adv. Chem. Phys.*, 1991, **80**, 127–199.
153 G. Peintler, ZiTa, Version 5.0, a Comprehensive Program Package for Fitting Parameters of Chemical Reaction Mechanism, Attila József University, Szeged, Hungary, 1998.
154 A. K. Horváth, I. Nagypál, G. Peintler, K. Kustin and I. R. Epstein, Kinetics and Mechanism of the Decomposition of Chlorous Acid, *J. Phys. Chem.*, submitted.
155 P. Ruoff, *J. Phys. Chem.*, 1984, **88**, 2851–2857.
156 F. Hynne and P. G. Sørensen, *J. Phys. Chem.*, 1987, **91**, 6573–6577.
157 A. Arkin and J. Ross, *J. Phys. Chem.*, 1995, **99**, 970–979.
158 M. W. Hirsch and S. Smale, *Differential Equations, Dynamical Systems and Linear Algebra*, Academic Press, New York, 1974.
159 G. Nicolis, *Introduction to Nonlinear Science*, Cambridge University Press, Cambridge, 1995.
160 A. S. Mikhailov and G. Ertl, *Science*, 1996, **272**, 1596–1597.
161 Y. Tabe and H. Yokoyama, *Langmuir*, 1995, **11**, 4609–4613.
162 R. J. Dylla and B. A. Korgel, *ChemPhysChem*, 2001, 62–64.
163 G. P. Misra and R. A. Siegel, *J. Controlled Release*, 2002, **81**, 1–6.
164 A. M. Khan and J. A. Pojman, *Trends Polym. Sci.*, 1996, **4**, 253–257.